

# APPARENT SLIP FOR AN UPPER CONVECTED MAXWELL FLUID

ANDREAS MÜNCH\*, BARBARA WAGNER†, L. PAMELA COOK‡, AND RICHARD R. BRAUN‡

**Abstract.** In this study the flow field of a nonlocal, diffusive upper convected Maxwell (UCM) fluid with a polymer in a solvent undergoing shearing motion is investigated for pressure driven planar channel flow and the free boundary problem of a liquid layer on a solid substrate. For large ratios of the zero shear polymer viscosity to the solvent viscosity, it is shown that channel flows exhibit boundary layers at the channel walls. In addition, for increasing stress diffusion the flow field away from the boundary layers undergoes a transition from a parabolic to a plug flow. Using experimental data for the wormlike micelle solutions CTAB/NaSal and CPyCl/NaSal, it is shown that the analytic solution of the governing equations predicts these signatures of the velocity profiles. Corresponding flow structures and transitions are found for the free boundary problem of a thin layer sheared along a solid substrate. Matched asymptotic expansions are used to first derive sharp-interface models describing the bulk flow with expressions for an *apparent slip* for the boundary conditions, obtained by matching to the flow in the boundary layers. For a thin film geometry several asymptotic regimes are identified in terms of the order of magnitude of the stress diffusion, and corresponding new thin film models with a slip boundary condition are derived.

**Key words.** Wormlike micelle solutions, thin-film approximation, sharp-interface limit, matched asymptotic expansions

**AMS subject classifications.** 76A05, 34E05, 76A20

**1. Introduction.** Slip at the liquid-solid interface is a common phenomenon when liquid polymer layers are sheared along solid substrates. On the micro- or nanoscale of the liquid bulk system, this condition can have important implications for the liquid flow structure. A well-documented example is a polymer film that dewets from a hydrophobically coated substrate. An effective boundary condition for such complex systems is often given in the form of a Navier-Slip condition, relating the lateral velocity along the substrate to the shear rate  $u = bu_z$ . The quantity  $b$  denotes an *apparent slip* length and encodes an underlying mesoscopic mechanism. For entangled polymer melts dewetting from a monolayer of polymer chains grafted on a substrate, such a mechanism is given by a coil-stretch transition into a disentangled state having much lower Rouse friction, and thus apparent viscosity, within a very thin layer near the substrate as has been shown by Brochard & De Gennes [6]. The underlying mesoscopic mechanisms are different for polymer-melt solid-substrate systems, some of which are described in the reviews by Lauga et al. [16] or in Léger [17].

For polymer solutions or dilute polymer emulsions, analysis of the motion of the polymer chains within the thin interfacial region between the solid and the polymer suggest higher shear rates and lower viscosity within the interfacial region leading to an apparent velocity discontinuity and hence to an *apparent slip*, as discussed in [2, 3, 7].

Further extensions of these studies regarding polymer-polymer apparent slip can be found in [1]. For a large class of colloidal suspensions apparent slip as well as shear banding are discussed in the review by Ballesta et al. [4]. For other complex liquids such as wormlike micellar solutions, slip also may relate to the occurrence of shear banding, which is closely related to a plateau region in the shear stress versus shear rate flow curve, which has been examined for example [11, 15, 18, 24, 26, 27, 28].

In channel flow experiments these wormlike micellar solutions show a thin band of high shear rate flow near the channel walls with a plug-like flow in the remaining portion of the channel [19] and shown in simulations of the Vasquez, Cook, McKinley (VCM) model [8]. The VCM model is a non-linear two species model constructed to account for the breaking and reforming of the wormlike micelles. The solution in the high shear rate band near the wall contains primarily short micelles, while in the center of the channel, the distribution of micellar lengths is close to equilibrium. Thus the shear banding can be loosely thought of as evidence of phase demixing. To understand and quantify the emergence and magnitude of apparent slip and also the transitions in flow structure for polymer solutions, we focus here on a model system much simpler than the VCM model, and employ an UCM model with stress diffusion [9] in a water solvent.

We address first the pressure driven planar channel flow, which has been investigated in [8]. After we formulate the boundary value problem in Section 2, we derive, in Section 3, an exact solution to the governing equations showing that the flow structures and transition in velocity profiles are controlled by two

\*Mathematical Institute, University of Oxford, Andrew Wiles Building, Woodstock Road, Oxford OX2 6GG, UK ([andreas.muench@maths.ox.ac.uk](mailto:andreas.muench@maths.ox.ac.uk)).

†Institute of Mathematics, Technical University Berlin, Str. des 17. Juni 136, 10623 Berlin, Germany ([bwagner@math.tu-berlin.de](mailto:bwagner@math.tu-berlin.de)), Weierstrass Institute, Mohrenstrasse 39, 10117 Berlin, Germany ([wagnerb@wias-berlin.de](mailto:wagnerb@wias-berlin.de)).

‡Department of Mathematical Sciences, University of Delaware, Newark DE 19716, USA, ([cook@udel.edu](mailto:cook@udel.edu), [rjbraun@udel.edu](mailto:rjbraun@udel.edu)).

parameters, the ratio of the solvent viscosity to the zero shear rate polymer viscosity and the non-dimensional stress diffusion parameter.

We then extend this analysis to the free boundary problems of a liquid layer shearing along a solid substrate in Section 4. We exploit the boundary layer flow structure to derive a reduced sharp-interface model with an *apparent slip* boundary conditions using matched asymptotic expansions. These sharp-interface models with an *apparent slip* form the basis for the derivation of new thin-film models governing the shape of the free surface for moderate to large slip lengths. These models are discussed in Section 5 together with a linear stability analysis yielding multiple relaxation modes for the for the case of large stress diffusion.

We conclude with a discussion of *apparent slip* on related problems in the context of dewetting liquid bi-layers in Section 6.

**2. Maxwell fluid with solvent and diffusion.** For convenience, we discuss two-dimensional flows throughout this study. The governing equations are those of an UCM fluid with stress diffusion [8, 9]. These equations are also visible within the VCM model for wormlike micellar solutions [27] by assuming that only one species of micelles is present.

The spatial coordinates and velocity are given by  $\mathbf{x}' = (x', z')$  and  $\mathbf{v}' = (u', w')$ , corresponding to the streamwise and cross-stream directions, respectively. Time is denoted with  $t'$ . Primes denote dimensional variables. Conservation of mass requires

$$(2.1a) \quad \nabla' \cdot \mathbf{v}' = 0.$$

For  $D_{t'} = \partial_{t'} + u' \partial_{x'} + w' \partial_{z'}$ , conservation of momentum can be written as

$$(2.1b) \quad \rho D_{t'} \mathbf{v}' = \nabla' \cdot \mathbf{\Pi}',$$

where

$$(2.1c) \quad \mathbf{\Pi}' = -p\mathbf{I} + \eta_s \dot{\gamma}' - \tau'_p$$

is the total stress,  $\dot{\gamma}' = \nabla' \mathbf{v}' + (\nabla' \mathbf{v}')^{\mathbf{t}}$  the strain rate and the superscript  $\mathbf{t}$  denotes the transpose. Here  $\tau'_p = -\mathbf{A}' + G_0 \mathbf{I}$  denotes the polymer stress, which is governed by

$$(2.1d) \quad \lambda \mathbf{A}'_{(1')} + \mathbf{A}' - G_0 \mathbf{I} - D_s \lambda \nabla'^2 \mathbf{A}' = 0.$$

The density is denoted by  $\rho$ , the solvent viscosity by  $\eta_s$ , and the zero shear viscosity of the solution by  $\eta_0$ . The latter is the sum of the solvent viscosity and the contribution  $\eta_p^0 = G_0 \lambda$  from the micelles, that is,  $\eta_0 = \eta_s + \eta_p^0$ , where  $\lambda$  is the relaxation time of the micelles and  $G_0$  is the shear modulus at zero strain rate. We denote the upper convected derivative of a quantity  $\mathbf{f}$  by

$$(2.1e) \quad \mathbf{f}_{(1')} = D_{t'} \mathbf{f} - (\nabla' \mathbf{v}')^{\mathbf{t}} \cdot \mathbf{f} - \mathbf{f} \cdot (\nabla' \mathbf{v}').$$

The addition of the stress diffusion term is discussed in [8, 9]. The boundary conditions for the problem are as follows. At  $z' = 0$ :

$$(2.1f) \quad \mathbf{v}' = \mathbf{0}$$

and, because of the diffusion term, we also need boundary conditions on the stress. We assume no flux of conformation across boundaries hence

$$(2.1g) \quad \partial_{z'} \mathbf{A}' = 0.$$

At the free surface  $z' = h'$ , we have

$$(2.1h) \quad \mathbf{v}' \cdot \nabla' F' + \partial_{t'} F' = 0,$$

where  $F'(x', h'(x', t'), t') = z' - h'(x', t') = 0$  defines the location of the free surface. This results in the kinematic condition

$$\partial_{t'} h' - u' \partial_{x'} h - w' = 0.$$

The normal stress balance at the free surface is

$$[[\mathbf{n}' \cdot \mathbf{\Pi}' \cdot \mathbf{n}']] = \kappa \sigma$$

where  $\kappa = \nabla' \cdot \mathbf{n}$  is the curvature of the surface and  $\sigma$  is the surface tension of the film/air interface. We define the jump in a function  $f'$  across the film/air interface as  $[[f']] = f'_{\text{air}} - f'_{\text{film}}$ . We further assume that the air is a passive gas with zero stress components and pressure. The tangential stress balance is given by

$$[[\mathbf{t}' \cdot \mathbf{\Pi}' \cdot \mathbf{n}']] = 0$$

at the surface. Due to the inclusion of stress diffusion we need a boundary condition on stress at the free surface. Using the no flux boundary conditions of conformation gives

$$\mathbf{n}' \cdot \nabla' \mathbf{A}' = 0$$

on the free surface. In detail, the normal and tangential stress boundary conditions are, respectively,

$$-p' + \mathbf{n}' \cdot (\mathbf{A}' - G_0 \mathbf{I} + \eta_s \dot{\gamma}) \cdot \mathbf{n}' = \sigma \partial_{x'}^2 h' (N')^{-3},$$

and

$$[1 - (\partial_{x'} h')^2] [A_{xx} + \eta_s (\partial_{z'} u' + \partial_{x'} w')] - \partial_{x'} h' (A'_{xx} + 2\eta_s \partial_{x'} u') + \partial_{x'} h' (A'_{zz} + 2\eta_s \partial_{z'} w') = 0.$$

We have made use of

$$\mathbf{n}' = (-\partial_{x'} h' \mathbf{i} + \mathbf{j})(N')^{-1}, \quad \mathbf{t}' = (\mathbf{i} + \partial_{x'} h' \mathbf{j})(N')^{-1}, \quad \text{and} \quad N'[1 + (\partial_{x'} h')^2]^{1/2}.$$

We non-dimensionalize the governing equations by setting

$$x' = \ell x, \quad z' = Hz, \quad h' = Hh, \quad u' = Uu, \quad w' = \epsilon U w, \quad t' = \frac{\ell}{U} t, \quad p' = \frac{G_0}{\epsilon} p, \quad \mathbf{A}' = G_0 \mathbf{A}.$$

Here  $H$  is the the characteristic thickness of the film,  $\ell$  the characteristic length along it.  $U$  the characteristic speed along the film. The following non-dimensional parameters arise:

$$\epsilon = \frac{H}{\ell}, \quad \text{Re} = \frac{\rho U H}{\eta_s}, \quad \text{De} = \frac{\lambda U}{H}, \quad \delta = \sqrt{\frac{D_s \lambda}{H^2}}, \quad \text{and} \quad \alpha = \sqrt{\frac{\delta}{\eta_p^0 / \eta_s}}.$$

Re is the Reynolds number, De is the Deborah number,  $\delta$  is the nondimensional stress diffusion parameter and  $D_t = \partial_t + u \partial_x + w \partial_z$ . We note that in this study, we scale the pressure larger than the polymer stress terms. However, other choices where pressure and polymer stress are of the same order may also become relevant. In the momentum equation we balance

$$\frac{\alpha^2}{\delta} \text{De} \partial_z^2 u \sim \partial_z A_{xx} \sim \partial_x p.$$

For the derivation of the lubrication problem with a free boundary, we require that at the free boundary the pressure  $p$  is balanced by surface tension. Hence, in the normal stress condition we let

$$S_p = \frac{\sigma \epsilon^3}{G_0 H} = O(1),$$

123 which means that

$$124 \quad \frac{\sigma H}{\ell^2} \sim \frac{G_0}{\epsilon} \quad \text{or} \quad \epsilon^3 \sim \frac{G_0 H}{\sigma}.$$

125 The nondimensional governing equations then become as follows. For conservation of mass,

$$126 \quad (2.4a) \quad \partial_x u + \partial_z w = 0.$$

128 For momentum conservation,

$$129 \quad (2.4b) \quad \epsilon \frac{\alpha^2}{\delta} \text{DeRe} D_t u = -\partial_x p + \frac{\alpha^2}{\delta} \text{De} (\epsilon^2 \partial_x^2 u + \partial_z^2 u) + \epsilon \partial_x A_{xx} + \partial_z A_{xz},$$

$$130 \quad (2.4c) \quad \epsilon^3 \frac{\alpha^2}{\delta} \text{DeRe} D_t w = -\partial_z p + \epsilon^2 \frac{\alpha^2}{\delta} \text{De} (\epsilon^2 \partial_x^2 w + \partial_z^2 w) + \epsilon (\epsilon \partial_x A_{xz} + \partial_z A_{zz}).$$

132 For the polymer part of the deviatoric stress, the equations are as follows:

$$133 \quad (2.4d) \quad \epsilon \text{De} (D_t A_{xx} - 2\epsilon^{-1} A_{xz} \partial_z u - 2\epsilon A_{xx} \partial_x u) + A_{xx} - 1 = \delta (\epsilon^2 \partial_x^2 A_{xx} + \partial_z^2 A_{xx}),$$

$$134 \quad (2.4e) \quad \epsilon \text{De} (D_t A_{xz} - \epsilon^{-1} A_{zz} \partial_z u - \epsilon A_{xx} \partial_x w) + A_{xz} = \delta (\epsilon^2 \partial_x^2 A_{xz} + \partial_z^2 A_{xz}),$$

$$135 \quad (2.4f) \quad \epsilon \text{De} (D_t A_{zz} - 2A_{zz} \partial_z w - 2\epsilon A_{xz} \partial_x w) + A_{zz} - 1 = \delta (\epsilon^2 \partial_x^2 A_{zz} + \partial_z^2 A_{zz}).$$

137 The boundary conditions are, at  $z = 0$ ,

$$138 \quad (2.4g) \quad u = w = 0 \quad \text{and} \quad \partial_z A_{ij} = 0,$$

140 with  $i = x, z$  and  $j = x, z$ . For the free surface boundary conditions at  $z = h(x, t)$  we have:

$$141 \quad (2.4h) \quad \partial_t h - u \partial_x h = w$$

$$142 \quad -S_p \partial_x^2 h N^{-3} = p + N^{-2} \left\{ -\epsilon [A_{zz} - 1 + \epsilon^2 (\partial_x h)^2 (A_{xx} - 1)] \right.$$

$$143 \quad \left. -2 \frac{\alpha^2}{\delta} \epsilon^2 \text{De} \partial_x h (\partial_z u + \epsilon^2 \partial_x w) \right.$$

$$144 \quad (2.4i) \quad \left. -2\epsilon \partial_x h A_{xz} + 2 \frac{\alpha^2}{\delta} \epsilon^2 \text{De} [\partial_z w + \epsilon^2 (\partial_x h)^2 \partial_x u] \right\},$$

$$145 \quad 0 = \epsilon \partial_x h (A_{zz} - A_{xx}) + A_{xz} [1 - \epsilon^2 (\partial_x h)^2] + \frac{\alpha^2}{\delta} \text{De} (\partial_z u + \epsilon^2 \partial_x w) [1 - \epsilon^2 (\partial_x h)^2]$$

$$146 \quad (2.4j) \quad -2 \frac{\alpha^2}{\delta} \text{De} \epsilon \partial_x h (\partial_x u - \partial_z w),$$

148 and

$$149 \quad (2.4k) \quad (\partial_z A_{ij} - \epsilon^2 \partial_x h \partial_x A_{ij}) N^{-1} = 0.$$

151 We have used

$$152 \quad (2.4l) \quad \mathbf{n} = (-\epsilon \partial_x h \mathbf{i} + \mathbf{j}) N^{-1}, \quad \mathbf{t} = (\mathbf{i} + \epsilon \partial_x h \mathbf{j}) N^{-1}, \quad \text{and} \quad N = [1 + (\epsilon \partial_x h)^2]^{1/2},$$

154 as well as

$$155 \quad (2.4m) \quad \overline{\text{Ca}} = \eta_0 U / \sigma \epsilon^3 \quad \text{and} \quad S_p = \sigma \epsilon^2 / G_0 \ell = \text{De} / \overline{\text{Ca}}.$$

157 **3. Boundary layers in planar channel flow.** To study the effect of the parameters  $\alpha$  and  $\delta$ , we first  
 158 consider the problem of planar channel flow, where we can find explicit solutions [8]. In this case, we normalize  
 159 with the width of the channel  $h$  so that the cross-stream variable is  $-1/2 < z < 1/2$ . The boundary conditions  
 160 at each side wall ( $z = \pm 1/2$ ) are those of no slip,  $u = 0$ , and no flux of conformation/stress,  $\partial_z A_{ij} = 0$  with  
 161  $i = x, z$  and  $j = x, z$ . Consistent with parallel shear flow, we assume that  $w = 0$  and that  $\partial_x p$  and all other  
 162 variables are independent of  $x$ . We then obtain from (2.4f) and (2.4g) that  $A_{zz} = 1$ . Using this in (2.4e),  
 163 solving for  $\partial_z u$ , inserting the result into (2.4b) and integrating the latter once, we obtain

$$164 \quad (3.1) \quad \frac{\alpha^2}{1 + \alpha^2/\delta} \partial_z^2 A_{xz} - A_{xz} = -\frac{1}{1 + \alpha^2/\delta} (z - c) \partial_x p.$$

165 The constant of integration  $c = 0$  can be set to zero if we assume the flow field is symmetric about  $z = 0$ ,  
 166 that is,  $u$  is an even function in  $z$ . Integrating (3.1) and using (2.4g) gives

$$167 \quad (3.2) \quad A_{xz} = \frac{\partial_x p}{1 + \alpha^2/\delta} \left[ \hat{z} - \frac{\alpha}{\sqrt{1 + \alpha^2/\delta}} \frac{\sinh\left(\sqrt{1 + \alpha^2/\delta} \frac{\hat{z}}{\alpha}\right)}{\cosh\left(\sqrt{1 + \alpha^2/\delta} \frac{1}{2\alpha}\right)} \right].$$

168 Substituting into the first integral of the momentum equation gives the velocity component along the channel:  
 169

$$170 \quad (3.3a) \quad u = -\frac{\partial_x p}{\text{De}} \frac{1}{1 + \alpha^2/\delta} (T_1 + T_2),$$

171 where

$$172 \quad (3.3b) \quad T_1 = -\left(\frac{\hat{z}^2}{2} - \frac{1}{8}\right), \quad \text{and} \quad T_2 = \frac{\delta}{1 + \alpha^2/\delta} \left[ 1 - \frac{\cosh\left(\sqrt{1 + \alpha^2/\delta} \frac{\hat{z}}{\alpha}\right)}{\cosh\left(\sqrt{1 + \alpha^2/\delta} \frac{1}{2\alpha}\right)} \right].$$

173 This velocity distribution can develop boundary layers and plug flow depending on the sizes of  $\alpha$  and  $\delta$ .  
 174 To see this, we consider the two terms  $T_1$  and  $T_2$  in (3.3) for fixed channel width. First consider  $\alpha$  and the  
 175 no-slip boundary condition; a boundary layer occurs when  $\alpha$  in the cosh's in  $T_2$  is small,

$$176 \quad (3.4) \quad \alpha \ll 1.$$

177 For  $\alpha \ll 1$  and  $|z| < 1/2$  fixed,  $T_2 \rightarrow \delta$  which will not satisfy a no-slip boundary condition. On the other  
 178 hand,  $\hat{z} \rightarrow \pm 1/2$  for fixed  $\alpha$  leads to  $T_2 \rightarrow 0$ , which does satisfy the no-slip requirement; the different limits  
 179 imply that boundary layers occur in  $T_2$  at  $z = \pm 1/2$ . The transition to plug-flow behavior is possible if the  
 180 parabolic velocity profile from the first term  $T_1$  does not contribute significantly to the flow, which is the  
 181 case if  $\delta \gg 1$ .

182 Fig. 1 shows the flow field  $u$  for several choices of  $\delta$  and  $\alpha$ ; we normalized with its maximum for ease of  
 183 comparison. Fig. 1 shows plots for  $\delta = 0.1, 1$  and  $10$ ; in each plot,  $u$  is plotted for three different values of  
 184  $\alpha$  (dotted,  $2.2 \times 10^{-2}$ ; dashed,  $7.1 \times 10^{-3}$ ; solid,  $2.2 \times 10^{-3}$ ). In all cases  $u = 0$  at the boundary, but as  $\alpha$   
 185 decreases, a boundary layer becomes more apparent at each value of  $\delta$ . The insets shows an enlarged view  
 186 of the plots near  $z = 1/2$ , and it is clearly seen that a boundary layer develops as  $\alpha$  decreases. In particular  
 187 in the inset of the middle and the figure on the bottom, the width of the layer decreases by about the same  
 188 factor as  $\alpha$  and is in fact largely independent of  $\delta$  as expected from  $T_2$  in (3.3). The boundary layers in the  
 189 left sub-figure are less obvious as the parabolic contribution  $T_1$ , which does not have boundary layers of its  
 190 own, dominates the appearance of the flow profile for small  $\delta$ .  $\delta > 0$  is needed to have boundary layers, and  
 191 therefore these layers only develop in the presence of stress diffusion. We note that fixed  $\delta$  with decreasing  
 192  $\alpha$  implies increasing the polymer-to-solvent viscosity ratio  $\eta_p^0/\eta_s$ .

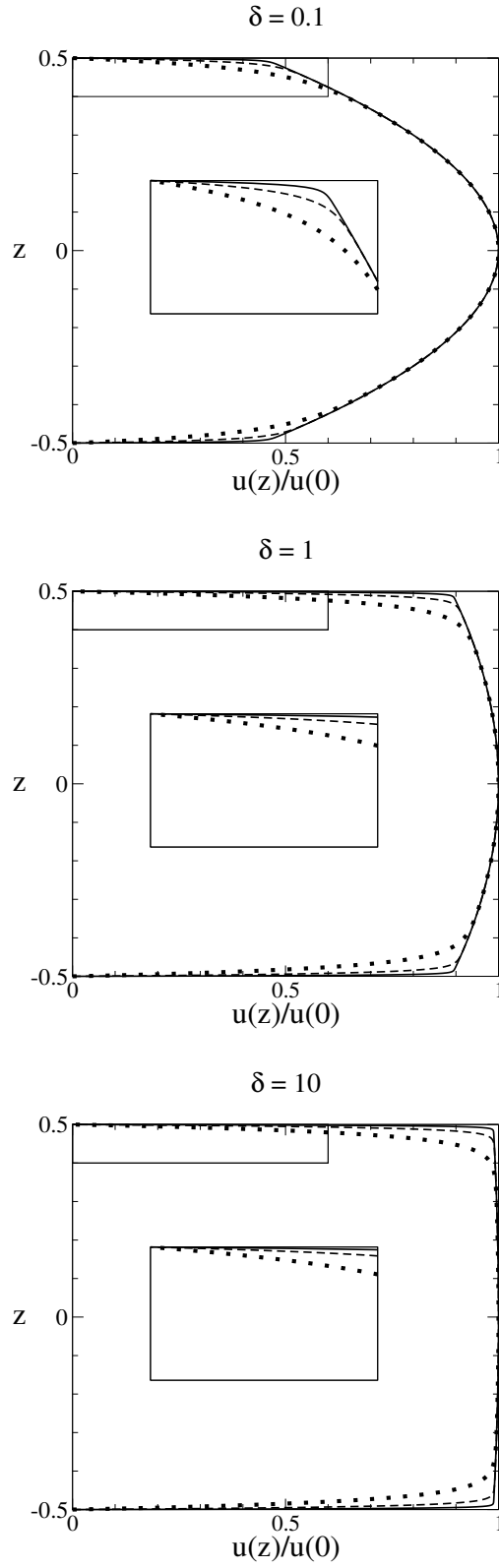


FIG. 1. Velocity profiles for different  $\delta = 0.1, 1, 10$  as shown in the title from top to bottom, and for different  $\alpha = 2.2 \times 10^{-2}, 7.1 \times 10^{-3}, 2.2 \times 10^{-3}$ , shown in each sub-figure by a dotted, dashed and solid line, respectively. For clarity, we enlarged in each sub-figure the boundary layer region in an inset.

193 We now compare velocity profiles for the same  $\alpha$  but different  $\delta$ , that is, for  $\delta = 0.1, 1$  and  $10$ . We observe  
 194 that the parabolic profile that is present for the smaller  $\delta$  flattens out for  $\delta = 1$  and becomes a plug-flow  
 195 profile for  $\delta = 10$ , or more generally, for large  $\delta$ . This plug flow only develops with substantial stress diffusion  
 196 across the channel. Indeed,  $\delta \gg 1$  implies  $H \ll \sqrt{D_s \lambda}$  (see (2.3)). For the physical parameters obtained  
 197 from [5] and given in Table 1 and its caption,  $\sqrt{D_s \lambda}$  is in the range of  $10 \dots 100 \mu\text{m}$  and therefore plug-flow  
 198 situations are only relevant for channel widths of tens of microns or smaller. Thus we emphasize that both  
 199 the formation of boundary layers and the transition to plug flow is linked to the presence of stress diffusion.

200 As an example we show some typical parameter values for CTAB/NaSal and CPyCl/NaSal solutions  
 201 of different concentrations and channel widths in Table 1 and the corresponding velocity profiles in Fig. 2.  
 202 Again, the results are scaled to have unit size flow domain in  $|z| < 1/2$  (the actual channel width  $H$  enters  
 203 through the non-dimensional parameters) and normalised by  $u(0)$ . For each solution and concentration, the  
 204 profiles are shown for two choices of  $H$ . Since both  $\delta$  and  $\alpha$  increase with  $H$ , the curvature of the profile near  
 205 the center of the channel and the width of the boundary layer change simultaneously, with the more plug-like  
 206 flow and wider boundary layers occurring for the smaller  $H$ . The profiles typically have a visible curvature,  
 207 with a distinctive plug flow behaviour with thin boundary layers occurring only for the largest  $\delta$  in table 1, see  
 208 rows 3 (corresponds to rightmost solid line in left sub-figure) and 8 (corresponds to rightmost dashed line in  
 209 the right sub-figure). Notice that the relaxation time  $\lambda$  decreases with concentration for CPyCl/NaSal but  
 210 decreases dramatically for CTAB/NaSal, and therefore the trends in  $\delta$  are also reversed.

211 Returning to consider a fixed  $\delta > 0$ , we note that the asymptotic structure of the flow for  $\alpha$  can be used  
 212 to interpret the effect of  $\delta$  as a slip length on the outer solution i.e. at an  $O(1)$  distance from the walls. The  
 213 leading order outer solution is obtained by taking the limit  $\alpha \rightarrow 0$  in (3.3) for fixed  $\delta$  and  $z$ , with  $|z| < 1/2$ ,  
 214 giving

$$215 \quad (3.5) \quad u = -\frac{\partial_x p}{\text{De}} \left\{ -\left( \frac{z^2}{2} - \frac{1}{8} \right) + \delta \right\}.$$

216 Interestingly, the resulting flow profile has the same parabolic form as for a Newtonian flow in a channel  
 217 except that it does not satisfy the no-slip condition at  $z = \pm 1/2$ . The finite slip velocity at the walls can be  
 218 used to define a slip length via the Navier-slip condition

$$219 \quad (3.6) \quad \left. \frac{|u|}{|u_z|} \right|_{z=\pm 1/2} = 2\delta,$$

220 suggesting a slip length of  $2\delta$ .

221 If we now consider the sub-limit  $\delta \gg 1$ , we expect to see the shear stress at the wall to drop to zero and  
 222 thus the development of plug flow. Indeed, if we rescale  $u = \delta \bar{u}$ , we get in the limit  $\delta \rightarrow \infty$  that

$$223 \quad (3.7) \quad \bar{u} = -\frac{\partial_x p}{\text{De}}$$

224 which is constant in  $z$ .

225 For this upper convected Maxwell model, we have shown that the limit of small  $\alpha$ , corresponding to small  
 226 solvent viscosity, results in boundary layers at the walls of the channel. Furthermore, for large  $\delta$ , corresponding  
 227 to thin films relative to the polymer stress diffusion length, plug flow develops in the interior of the channel.  
 228 We now move on to consider a thin film with a deforming free surface and use these results to approximate  
 229 the velocity field and polymer stress distribution inside the flowing fluid. With those approximate flow and  
 230 stress fields, we derive equations for the film thickness and leading order polymer stress in different limits.

231 **4. Sharp-interface limit for the free boundary flow.** We now consider flow on the domain  $0 \leq$   
 232  $z \leq h(x, t)$  with overall dimensional thickness  $H$  as before. The free surface at  $z = h$  must be found as  
 233 part of the problem as is typical, and there is still a no-slip and impenetrable substrate at  $z = 0$ . We derive  
 234 a sharp-interface model in the limit  $\alpha \rightarrow 0$  for the scaled full governing equations (2.4) including the free  
 235 boundary at  $z = h$ , leaving  $\varepsilon$  and  $\delta$  fixed. This approach leads to an outer problem for which matching to the  
 236 bottom boundary layer at the substrate at  $z = 0$  results in a Navier-slip-like condition. The leading order  
 237 outer problem can then be passed through the thin film limit  $\varepsilon \rightarrow 0$  in the following section, with different  
 238 cases for the different regimes of  $\delta$ .

CTAB/NaSal	$G_0$	$\lambda$	$\eta_0$	$U$	$S_p$	Re	De	$H$	$\delta$	$\alpha$
25/25	2.5	27	68	1.5e-7	1.5e-6	1.5e-6	4.0e-2	1e-4	1.6	4.9e-3
150/150	94.8	0.4	38	2.6e-7	2.6e-6	2.6e-6	1.1e-3	1e-4	2.0e-1	2.3e-3
25/25	2.5	27	68	1.5e-7	1.5e-6	1.5e-6	4.0e-1	1e-5	16	1.6e-2
150/150	94.8	0.4	38	2.6e-7	2.6e-6	2.6e-6	1.1e-2	1e-5	2	7.3e-3
CpyCl/NaSal	$G_0$	$\lambda$	$\eta_0$	$U$	$S_p$	Re	De	$H$	$\delta$	$\alpha$
50/25	4.2	7.7e-1	2.8	3.5e-6	3.1e-5	3.1e-5	2.7e-2	1e-4	2.8e-1	9.9e-3
200/100	100	1.7	200	5.1e-8	5.7e-7	5.7e-7	8.6e-4	1e-4	4.1e-1	1.4e-3
50/25	4.2	7.7e-1	2.8	3.5e-6	3.1e-5	3.1e-5	2.7e-1	1e-5	2.8	3.1e-2
200/100	100	1.7	200	5.1e-8	5.7e-7	5.7e-7	8.6e-3	1e-5	4.1	4.6e-3

TABLE 1

Parameter values for CTAB/NaSal (top) and for CPyCl/NaSal (bottom) solutions at different concentrations in mM and for two layer thicknesses  $H$ . The values are obtained from A. Bhardwaj, E. Miller, and J. P. Rothstein, *J of Rheology*, 51:693-719 (2007) [5]. The units for  $\lambda$ ,  $U$  and  $H$  are s and m/s and m, respectively. Here  $\rho = 10^3 \text{ kg/m}^3$  and  $U$  is chosen by making  $\overline{Ca} = 1$ ,  $D_s = 10^{-9} \text{ m}^2/\text{s}$  and  $\eta_s = 10^{-3} \text{ kg/m.s}$ . Note that  $\overline{Ca} = 1$  enforces  $S_p = \text{Re}$ .

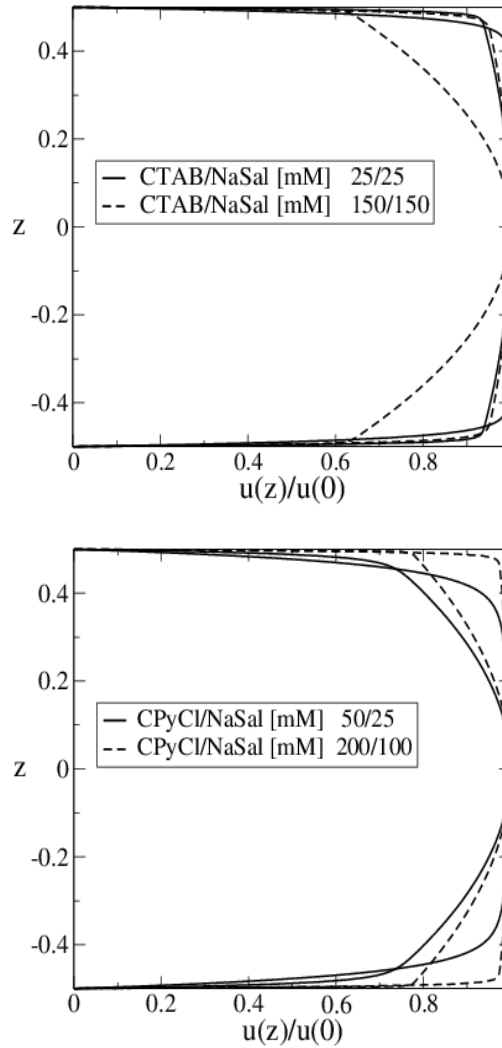


FIG. 2. Velocity profiles for different ratios concentrations of CTAB/NaSal and CPyCl/NaSal solutions and channel widths as given in Table 1.  $H$  is smaller for the velocity profiles that are closer to plug flow near  $z = 0$ .



239 **4.1. Outer problem.** We first treat the flow away from the boundaries. We assume the outer variables  
 240 depend on  $x$ ,  $z$  and  $t$ , and that they can be expanded in a regular expansion in  $\alpha$ :

$$\begin{aligned} 241 \quad u &= u^{(0)} + \alpha u^{(1)} + \dots, & p &= p^{(0)} + \alpha p^{(1)} + \dots \\ 242 \quad w &= w^{(0)} + \alpha w^{(1)} + \dots, & A_{ij} &= A_{ij}^{(0)} + \alpha A_{ij}^{(1)} + \dots \end{aligned}$$

243 Then, to leading order in  $\alpha$  mass and momentum conservation become

$$\begin{aligned} 244 \quad (4.2a) \quad & 0 = \partial_x u^{(0)} + \partial_z w^{(0)} \\ 245 \quad (4.2b) \quad & 0 = -\partial_x p^{(0)} + \epsilon \partial_x A_{xx}^{(0)} + \partial_z A_{xz}^{(0)}, \\ 246 \quad (4.2c) \quad & 0 = -\partial_z p^{(0)} + \epsilon \left( \partial_x A_{xz}^{(0)} + \partial_z A_{zz}^{(0)} \right). \end{aligned}$$

247 For the polymer part of the deviatoric stress, the equations are as follows:

$$\begin{aligned} 248 \quad (4.2d) \quad \epsilon \text{De} \left( D_t A_{xx}^{(0)} - 2\epsilon^{-1} A_{xz}^{(0)} \partial_z u^{(0)} - 2A_{xx}^{(0)} \partial_x u^{(0)} \right) + A_{xx}^{(0)} - 1 &= \delta \left( \epsilon^2 \partial_x^2 A_{xx}^{(0)} + \partial_z^2 A_{xx}^{(0)} \right), \\ 249 \quad (4.2e) \quad \epsilon \text{De} \left( D_t A_{xz}^{(0)} - \epsilon^{-1} A_{zz}^{(0)} \partial_z u^{(0)} - \epsilon A_{xx}^{(0)} \partial_x w^{(0)} \right) + A_{xz}^{(0)} &= \delta \left( \epsilon^2 \partial_x^2 A_{xz}^{(0)} + \partial_z^2 A_{xz}^{(0)} \right), \\ 250 \quad (4.2f) \quad \epsilon \text{De} \left( D_t A_{zz}^{(0)} - 2A_{zz}^{(0)} \partial_z w^{(0)} - 2\epsilon A_{xz}^{(0)} \partial_x w^{(0)} \right) + A_{zz}^{(0)} - 1 &= \delta \left( \epsilon^2 \partial_x^2 A_{zz}^{(0)} + \partial_z^2 A_{zz}^{(0)} \right). \end{aligned}$$

251 The boundary conditions at  $z = 0$  and  $z = h$  need to be obtained from matching to solutions of appropriate  
 252 boundary layer problems.

253 **4.2. Inner problem at the substrate.** At  $z = 0$  the highest  $z$ -derivatives of  $u$  have dropped out. For  
 254 the boundary layer there, we introduce the ‘‘inner’’ independent variable

$$255 \quad \zeta = \frac{z}{\alpha}.$$

256 The inner dependent variables are denoted by  $\tilde{u}$ ,  $\tilde{w}$ ,  $\tilde{p}$  and  $\tilde{A}_{ij}$  and the inner problem is now

$$\begin{aligned} 257 \quad (4.3a) \quad \epsilon \frac{\alpha^2}{\delta} \text{DeRe} D_t \tilde{u} &= -\partial_x \tilde{p} + \frac{1}{\delta} \text{De} \left( \alpha^2 \epsilon^2 \partial_x^2 \tilde{u} + \partial_\zeta^2 \tilde{u} \right) + \epsilon \partial_x \tilde{A}_{xx} + \frac{1}{\alpha} \partial_\zeta \tilde{A}_{xz}, \\ 258 \quad (4.3b) \quad \epsilon^3 \frac{\alpha^2}{\delta} \text{DeRe} D_t \tilde{w} &= -\frac{1}{\alpha} \partial_\zeta \tilde{p} + \epsilon^2 \frac{1}{\delta} \text{De} \left( \alpha^{*2} \epsilon^2 \partial_x^2 \tilde{w} + \partial_\zeta^2 \tilde{w} \right) + \epsilon \left( \epsilon \partial_x \tilde{A}_{xz} + \frac{1}{\alpha} \partial_\zeta \tilde{A}_{zz} \right), \end{aligned}$$

259

$$\begin{aligned} 260 \quad (4.4a) \quad \epsilon \text{De} \left( D_t \tilde{A}_{xx} - \frac{2}{\epsilon \alpha} \tilde{A}_{xz} \partial_\zeta \tilde{u} - 2\tilde{A}_{xx} \partial_x \tilde{u} \right) + \tilde{A}_{xx} - 1 &= \delta \left( \epsilon^2 \partial_x^2 \tilde{A}_{xx} + \frac{1}{\alpha^2} \partial_\zeta^2 \tilde{A}_{xx} \right), \\ 261 \quad (4.4b) \quad \epsilon \text{De} \left( D_t \tilde{A}_{xz} - \frac{2}{\epsilon \alpha} \tilde{A}_{zz} \partial_\zeta \tilde{u} - \epsilon \tilde{A}_{xx} \partial_x \tilde{w} \right) + \tilde{A}_{xz} &= \delta \left( \epsilon^2 \partial_x^2 \tilde{A}_{xz} + \frac{1}{\alpha^2} \partial_\zeta^2 \tilde{A}_{xz} \right), \\ 262 \quad (4.4c) \quad \epsilon \text{De} \left( D_t \tilde{A}_{zz} - \frac{2}{\alpha} \tilde{A}_{zz} \partial_\zeta \tilde{w} - 2\epsilon \tilde{A}_{xz} \partial_x \tilde{w} \right) + \tilde{A}_{zz} - 1 &= \delta \left( \epsilon^2 \partial_x^2 \tilde{A}_{zz} + \frac{1}{\alpha^2} \partial_\zeta^2 \tilde{A}_{zz} \right). \end{aligned}$$

263 At  $\zeta = 0$ , the boundary conditions are

$$264 \quad (4.5) \quad \tilde{u} = \tilde{w} = 0 \quad \text{and} \quad \partial_\zeta \tilde{A}_{ij} = 0,$$

265 with  $i = x, \zeta$  and  $j = x, \zeta$ . We again expand the solution as a regular perturbation series in  $\alpha$ :

$$\begin{aligned} 266 \quad \tilde{u} &= \tilde{u}^{(0)} + \alpha \tilde{u}^{(1)} + \dots, & p &= \tilde{p}^{(0)} + \alpha \tilde{p}^{(1)} + \dots \\ 267 \quad \tilde{w} &= \tilde{w}^{(0)} + \alpha \tilde{w}^{(1)} + \dots, & A_{ij} &= \tilde{A}_{ij}^{(0)} + \alpha \tilde{A}_{ij}^{(1)} + \dots \end{aligned}$$

268 To leading order, the inner problem is

$$269 \quad (4.6a) \quad 0 = \partial_\zeta \tilde{w}^{(0)},$$

$$270 \quad (4.6b) \quad 0 = \partial_\zeta \tilde{A}_{xz}^{(0)},$$

$$271 \quad (4.6c) \quad 0 = -\partial_\zeta \tilde{p}^{(0)} + \varepsilon \partial_\zeta \tilde{A}_{zz}^{(0)},$$

$$272 \quad (4.6d) \quad 0 = \partial_\zeta^2 \tilde{A}_{xx}^{(0)},$$

$$273 \quad (4.6e) \quad 0 = \partial_\zeta^2 \tilde{A}_{xz}^{(0)},$$

$$274 \quad (4.6f) \quad 0 = \partial_\zeta^2 \tilde{A}_{zz}^{(0)},$$

276 with the boundary conditions at  $\zeta = 0$ :

$$277 \quad (4.6g) \quad \tilde{u}^{(0)} = \tilde{w}^{(0)} = 0 \quad \text{and} \quad \partial_\zeta \tilde{A}_{ij}^{(0)} = 0.$$

279 From (4.6a) and (4.6g),  $\tilde{w}^{(0)} = 0$ . From (4.6f) and (4.6g),  $\tilde{A}_{ij}^{(0)}$  is a function of  $x$  and  $t$  only. Hence from  
280 (4.6c),  $\tilde{p}^{(0)}$  is also independent of  $\zeta$ .

281 The next order problem can be written as

$$282 \quad (4.7a) \quad 0 = \partial_x \tilde{u}^{(0)} + \partial_\zeta \tilde{w}^{(1)},$$

$$283 \quad (4.7b) \quad 0 = -\partial_x \tilde{p}^{(0)} + \frac{\text{De}}{\delta} \partial_\zeta^2 \tilde{u}^{(0)} + \partial_\zeta \tilde{A}_{xz}^{(1)},$$

$$284 \quad (4.7c) \quad 0 = -\partial_\zeta \tilde{p}^{(1)} + \varepsilon \partial_\zeta \tilde{A}_{zz}^{(1)},$$

$$285 \quad (4.7d) \quad 0 = 2\text{De} \tilde{A}_{xz}^{(0)} \partial_\zeta \tilde{u}^{(0)} + \delta \partial_\zeta^2 \tilde{A}_{xx}^{(1)},$$

$$286 \quad (4.7e) \quad 0 = \text{De} \tilde{A}_{zz}^{(0)} \partial_\zeta \tilde{u}^{(0)} + \delta \partial_\zeta^2 \tilde{A}_{xz}^{(1)},$$

$$287 \quad (4.7f) \quad 0 = \delta \partial_\zeta^2 \tilde{A}_{zz}^{(1)}.$$

289 with the boundary conditions at  $\zeta = 0$

$$290 \quad (4.7g) \quad \tilde{u}^{(1)} = \tilde{w}^{(1)} = 0 \quad \text{and} \quad \partial_\zeta \tilde{A}_{ij}^{(1)} = 0.$$

292 From (4.7f) and (4.7g), we see that  $\tilde{A}_{zz}^{(1)}$  is a function of  $x$  and  $t$  only, and from (4.7c), the same follows for  
293  $\tilde{p}^{(1)}$ ; thus

$$294 \quad (4.8) \quad \tilde{A}_{zz}^{(1)} = \tilde{A}_{zz}^{(1)}(x, t), \quad \tilde{p}^{(1)} = \tilde{p}^{(1)}(x, t).$$

295 Differentiation (4.7b) with respect to  $\zeta$  and recalling that  $\tilde{p}^{(0)}$  is independent of  $\zeta$  we have

$$296 \quad (4.9) \quad 0 = \frac{1}{\delta} \text{De} \partial_\zeta^3 \tilde{u}^{(0)} + \partial_\zeta^2 \tilde{A}_{xz}^{(1)};$$

297 using this in (4.7e), we find

$$298 \quad (4.10) \quad 0 = \tilde{A}_{zz}^{(0)} \partial_\zeta \tilde{u}^{(0)} - \partial_\zeta^3 \tilde{u}^{(0)}.$$

299 Since the  $\tilde{A}_{ij}^{(0)}$  are independent of  $\zeta$ , integrating once gives

$$300 \quad (4.11) \quad \partial_\zeta^2 \tilde{u}^{(0)} - \tilde{A}_{zz}^{(0)} \tilde{u}^{(0)} = c_1(x, t),$$

301 and for  $\tilde{A}_{zz}^{(0)} > 0$ , we obtain

$$302 \quad (4.12) \quad \tilde{u}^{(0)} = -\frac{c_1}{\tilde{A}_{zz}^{(0)}} + c_2 \exp\left(-\sqrt{\tilde{A}_{zz}^{(0)}} \zeta\right).$$

303 Here we excluded the exponentially growing part, since it does not match to the outer solution. Using the  
 304 boundary conditions (4.6g) yields  $c_2 = c_1/\tilde{A}_{zz}^{(0)}$  and hence

$$305 \quad (4.13) \quad \tilde{u}^{(0)} = \frac{c_1}{\tilde{A}_{zz}^{(0)}} \left( -1 + \exp \left( -\sqrt{\tilde{A}_{zz}^{(0)}} \zeta \right) \right).$$

306 Using this in (4.7b) gives

$$307 \quad \tilde{A}_{xz}^{(1)} = d_1(x, t) + \zeta \partial_x \tilde{p}^{(0)} - \frac{1}{\delta} \text{De} \partial_\zeta \tilde{u}^{(0)} \\ 308 \quad (4.14) \quad = d_1(x, t) + \zeta \partial_x \tilde{p}^{(0)} + \frac{1}{\delta} \text{De} \frac{c_1}{\sqrt{\tilde{A}_{zz}^{(0)}}} \exp \left( -\sqrt{\tilde{A}_{zz}^{(0)}} \zeta \right)$$

309 Due to the last equation in (4.7g), we have

$$310 \quad (4.15) \quad \partial_x \tilde{p}^{(0)} - \frac{1}{\delta} \text{De} c_1 = 0 \quad \text{or} \quad c_1 = \delta \frac{\partial_x \tilde{p}^{(0)}}{\text{De}},$$

311 so that

$$312 \quad (4.16a) \quad \tilde{u}^{(0)} = -\delta \frac{\partial_x \tilde{p}^{(0)}}{\text{De} \tilde{A}_{zz}^{(0)}} \left[ 1 - \exp \left( -\sqrt{\tilde{A}_{zz}^{(0)}} \zeta \right) \right],$$

$$313 \quad (4.16b) \quad \tilde{A}_{xz}^{(1)} = d_1(x, t) + \zeta \partial_x \tilde{p}^{(0)} + \frac{\partial_x \tilde{p}^{(0)}}{\sqrt{\tilde{A}_{zz}^{(0)}}} \exp \left( -\sqrt{\tilde{A}_{zz}^{(0)}} \zeta \right).$$

314 Notice that  $w^{(1)}$  can now be obtained by introducing (4.16a) into (4.7a) and using the boundary conditions  
 315 (4.7g). However,  $\tilde{A}_{zz}^{(0)}$  depends on  $x$  so the differentiation in (4.7a) creates a rather complicated expression that  
 316 we do not need in this paper; we omit the explicit result here. For similar reasons, we also skip determining  
 317  $\tilde{A}_{xx}^{(1)}$ , which can in principle be obtained from (4.7e), (4.16), and (4.7g).

318 Matching outer solution (at  $z = 0$ ) to the inner (as  $\zeta \rightarrow \infty$ ) yields the following boundary conditions for  
 319 the leading order outer problem (4.2):

$$320 \quad (4.17a) \quad p|_{z=0} = \tilde{p}^{(0)},$$

$$321 \quad (4.17b) \quad A_{ij}|_{z=0} = \tilde{A}_{ij}^{(0)},$$

$$322 \quad (4.17c) \quad u|_{z=0} = -\delta \frac{\partial_x p|_{z=0}}{\text{De} A_{zz}^{(0)}|_{z=0}},$$

$$323 \quad (4.17d) \quad w|_{z=0} = 0,$$

$$324 \quad (4.17e) \quad \partial_z A_{zz}^{(0)}|_{z=0} = 0,$$

$$325 \quad (4.17f) \quad \partial_z A_{xz}^{(0)}|_{z=0} = \partial_x p|_{z=0}.$$

326 **4.2.1. Inner problem at the free surface.** We now consider the inner layer near  $z = h$ . Introducing  
 327 inner variables via  $z = h - \alpha\zeta$  yields, to leading order in the bulk

$$328 \quad (4.18a) \quad \partial_x h \partial_\zeta \tilde{u}^{(0)} - \partial_\zeta \tilde{w}^{(0)} = 0,$$

$$329 \quad (4.18b) \quad -\partial_x h \partial_\zeta \tilde{p}^{(0)} + \varepsilon \partial_x h \partial_\zeta \tilde{A}_{xx}^{(0)} - \partial_\zeta \tilde{A}_{xz}^{(0)} = 0,$$

$$330 \quad (4.18c) \quad \partial_\zeta \tilde{p}^{(0)} + \varepsilon^2 \partial_x h \partial_\zeta \tilde{A}_{xz}^{(0)} - \varepsilon \partial_\zeta \tilde{A}_{zz}^{(0)} = 0,$$

$$331 \quad (4.18d) \quad \partial_\zeta^2 \tilde{A}_{xx}^{(0)} = 0,$$

$$332 \quad (4.18e) \quad \partial_\zeta^2 \tilde{A}_{xz}^{(0)} = 0,$$

$$333 \quad (4.18f) \quad \partial_\zeta^2 \tilde{A}_{zz}^{(0)} = 0.$$

334 Rescaling and retaining the leading order contributions for the boundary condition at  $z = h$  yields

$$335 \quad (4.19a) \quad \partial_t h + \tilde{u}^{(0)} \partial_x h = \tilde{w}^{(0)}$$

$$336 \quad -S_p \frac{\partial_x^2 h}{[1 + \epsilon^2 (\partial_x h)^2]^{3/2}} = \tilde{p}^{(0)} + \frac{1}{1 + \epsilon^2 h_x^2} \left\{ -\epsilon \left[ \tilde{A}_{zz}^{(0)} - 1 + \epsilon^2 (\partial_x h)^2 (\tilde{A}_{xx}^{(0)} - 1) \right] \right.$$

$$337 \quad (4.19b) \quad \left. + 2\epsilon^2 \partial_x h \tilde{A}_{xz}^{(0)} \right\},$$

$$338 \quad (4.19c) \quad 0 = \epsilon \partial_x h \left( \tilde{A}_{zz}^{(0)} - \tilde{A}_{xx}^{(0)} \right) + \tilde{A}_{xz}^{(0)} \left[ 1 - \epsilon^2 (\partial_x h)^2 \right]$$

$$339 \quad (4.19d) \quad \partial_\zeta \tilde{A}_{ij}^{(0)} = 0.$$

341 Integrating (4.18a) with respect to  $\zeta$  and using (4.19a) results in

$$342 \quad (4.20) \quad \partial_t h + \tilde{u}^{(0)} \partial_x h = \tilde{w}^{(0)}$$

343 for all  $\zeta \geq 0$ . the integration constants. Matching this to the outer thus imposes condition (4.19a) onto  
344 the leading order outer variables. Integrating (4.18d)-(4.18f) together with (4.19d) shows that the  $\tilde{A}_{ij}^{(0)}$  are  
345 independent of  $\zeta$ ,

$$346 \quad (4.21) \quad \tilde{A}_{ij}^{(0)} = \tilde{A}_{ij}^{(0)}(x, t).$$

347 Inserting this into (4.18c) gives similarly that  $\tilde{p}^0$  is independent of  $\zeta$

$$348 \quad (4.22) \quad \tilde{p}^{(0)} = \tilde{p}^{(0)}(x, t).$$

349 These four functions of  $x$  and  $t$  need to satisfy the boundary conditions (4.19b) and (4.19c), which matching  
350 then passes on to the leading order outer problem. Summarising, we obtain the following conditions at  $z = h$   
351 for the leading order outer variables  $u^{(0)}$ ,  $w^{(0)}$ ,  $A_{ij}^{(0)}$  and  $p^{(0)}$  (without the tilde),

$$352 \quad (4.23a) \quad \partial_t h + u^{(0)} \partial_x h = w^{(0)},$$

$$353 \quad -S_p \frac{\partial_x^2 h}{[1 + \epsilon^2 (\partial_x h)^2]^{3/2}} = p^{(0)} + \frac{1}{1 + \epsilon^2 h_x^2} \left\{ -\epsilon \left[ A_{zz}^{(0)} - 1 + \epsilon^2 (\partial_x h)^2 (A_{xx}^{(0)} - 1) \right] \right.$$

$$354 \quad (4.23b) \quad \left. + 2\epsilon^2 \partial_x h A_{xz}^{(0)} \right\},$$

$$355 \quad (4.23c) \quad 0 = \epsilon \partial_x h \left( A_{zz}^{(0)} - A_{xx}^{(0)} \right) + A_{xz}^{(0)} \left[ 1 - \epsilon^2 (\partial_x h)^2 \right].$$

357 We are now ready to proceed to deriving a thin film flow models.

358 **5. Thin film models.** In this section, we derive thin film models for the limit of small film thickness  
359  $\epsilon \ll 1$ . We consider two cases: one with moderate stress diffusion where  $\delta = O(1)$  fixed with respect to  $\epsilon$  and  
360  $\alpha$ , and the other for large stress diffusion  $\delta \gg 1$ .

361 **5.1. Moderate stress diffusion.** We first derive a thin film equation from the sharp interface model;  
362 the result shows that singular slip arises in that case. We then re-derive the result from the full model, in  
363 order to verify that the slip occurs independent of the order of the limits taken.

364 **5.1.1. Derivation from the sharp interface limit.** Taking the limit  $\epsilon \ll 1$  for the sharp-interface  
365 model (4.2) together with (4.17c), (4.17e), (4.23a), (4.23b) and (4.23c) yields, to leading order in  $\epsilon$  with

366  $\delta = O(1)$  fixed, the problem to solve on  $0 < z < h$  is

$$367 \quad (5.1a) \quad -\partial_x p + \partial_z A_{xz} = 0,$$

$$368 \quad (5.1b) \quad \partial_z p = 0,$$

$$369 \quad (5.1c) \quad -2\text{De}A_{xz}\partial_z u + A_{xx} - 1 = \delta \partial_z^2 A_{xx},$$

$$370 \quad (5.1d) \quad -\text{De}A_{zz}\partial_z u + A_{xz} = \delta \partial_z^2 A_{xz},$$

$$371 \quad (5.1e) \quad A_{zz} - 1 = \delta \partial_z^2 A_{zz},$$

$$372 \quad (5.1f) \quad \partial_x u + \partial_z w = 0.$$

373 We apply the following at  $z = 0$  :

$$374 \quad (5.1g) \quad u = -\delta \frac{\partial_x p}{\text{De}A_{zz}}, \quad w = 0,$$

$$375 \quad (5.1h) \quad \partial_z A_{zz} = 0;$$

376 and at  $z = h$  :

$$377 \quad (5.1i) \quad \partial_t h + u \partial_x h = w,$$

$$378 \quad (5.1j) \quad p = -S_p \partial_x^2 h,$$

$$379 \quad (5.1k) \quad A_{xz} = 0,$$

$$380 \quad (5.1l) \quad \partial_z A_{zz} = 0.$$

381 Note that (5.1l) arises from matching and it is derived in the appendix. We have dropped the superscript  
382 “(0)” from the variables for convenience.

383 Using (5.1b) and (5.1j) gives

$$384 \quad (5.2) \quad p = p(x, t) = -S_p \partial_x^2 h.$$

385 From (5.1a) we have

$$386 \quad (5.3) \quad \partial_z A_{xz} = -S_p \partial_x^3 h,$$

387 and from (5.1k)

$$388 \quad (5.4) \quad A_{xz} = S_p (h - z) \partial_x^3 h.$$

389 Integrating (5.1e) and using (5.1h) and (5.1l) results in

$$390 \quad (5.5) \quad A_{zz} = 1.$$

391 Then from (5.1d),

$$392 \quad (5.6) \quad \text{De} \partial_z u = -\delta \partial_z^2 A_{xz} + A_{xz} = S_p (h - z) \partial_x^3 h.$$

393 Using (5.1g), (5.2) and  $A_{zz} = 1$  gives the following boundary condition at  $z = 0$ :

$$394 \quad (5.7) \quad u = \frac{\delta S_p}{\text{De}} \partial_x^3 h.$$

395 From this and (5.6),

$$396 \quad (5.8) \quad u = \frac{S_p}{\text{De}} \partial_x^3 h \left( zh - \frac{z^2}{2} + \delta \right).$$

397 If we assume  $w|_{z=0} = 0$  then

$$398 \quad (5.9) \quad \partial_t h + \partial_x \int_0^h u dz = 0$$

399 holds and using (5.8), we obtain

$$400 \quad (5.10) \quad \partial_t h + \partial_x \left[ \frac{S_p}{\text{De}} \partial_x^3 h \left( \frac{h^3}{3} + \delta h \right) \right] = 0$$

401 This is a lubrication model with an  $h$ -dependent singular slip-length

$$402 \quad (5.11) \quad b = \frac{\delta}{h}$$

403 used by Greenspan [12] and derived in Huh & Scriven [13] and in Neogi & Miller [23]. This result illustrates  
404 how the apparent slip appears in the context of the nonlinear thin film equation, and that it is because there  
405 is a boundary layer in the velocity profile inside the film. However, one may ask whether this is because  
406  $\alpha \ll 1$  was taken prior to deriving the thin film equation. We address this point by deriving the same result  
407 from the full equations and taking the limit  $\alpha \ll 1$  after deriving a thin film equation.

408 **5.1.2. Derivation from the full governing equations.** We now directly derive a thin film model for  
409 the governing equations, where  $\alpha$  is treated as a fixed constant and  $\epsilon \ll 1$ .

410 For conservation of mass, we have

$$411 \quad (5.12a) \quad \partial_x u + \partial_z w = 0.$$

412 For momentum conservation,

$$413 \quad (5.12b) \quad 0 = -\partial_x p + \frac{\alpha^2}{\delta} \text{De} \partial_z^2 u + \partial_z A_{xz},$$

$$414 \quad (5.12c) \quad 0 = -\partial_z p.$$

415 For the polymer part of the deviatoric stress, the equations are as follows.

$$416 \quad (5.12d) \quad -2\text{De} A_{xz} \partial_z u + A_{xx} - 1 = \delta \partial_z^2 A_{xx},$$

$$417 \quad (5.12e) \quad -\text{De} A_{zz} \partial_z u + A_{xz} = \delta \partial_z^2 A_{xz},$$

$$418 \quad (5.12f) \quad A_{zz} - 1 = \delta \partial_z^2 A_{zz}.$$

419 Note that our choice of large pressure makes it larger than the leading order  $A_{zz}$  term.

420 The boundary conditions are, at  $z = 0$ ,

$$421 \quad (5.12g) \quad u = w = 0 \text{ and } \partial_z A_{ij} = 0,$$

422 with  $i = x, z$  and  $j = x, z$ .

423 On the free surface  $z = h$ ,

$$424 \quad (5.12h) \quad \partial_t h - u \partial_x h = w,$$

$$425 \quad (5.12i) \quad -S_p \frac{\partial_x^2 h}{[1 + \epsilon^2 (\partial_x h)^2]^{3/2}} = p,$$

$$426 \quad (5.12j) \quad A_{xz} + \frac{\alpha^2}{\delta} \text{De} \partial_z u = 0,$$

$$427 \quad (5.12k) \quad \partial_z A_{ij} = 0.$$

428 To solve this system, first consider  $A_{zz}$  since it is a linear equation. Applying the homogeneous Neumann  
429 boundary conditions (5.12g) and (5.12k) yields

$$430 \quad (5.13) \quad A_{zz} = 1,$$

431 i.e. the polymer stress state is uniform across the thin film. The polymer stress state for the other components  
432 will not be uniform in  $z$ . We integrate the momentum equation (5.12b) and use the tangential stress boundary  
433 condition (5.12k) as well as (5.13) to obtain

$$434 \quad (5.14) \quad \frac{\alpha^2}{\delta} \text{De} \partial_z u = -A_{xz} + (z - h) \partial_x p.$$

435 Now substituting for  $A_{zz}$  and  $\partial_z u$  in the polymer shear stress equation gives

$$436 \quad (5.15) \quad \frac{\alpha^2}{1 + \alpha^2/\delta} \partial_z^2 A_{xz} - A_{xz} = -\frac{1}{1 + \alpha^2/\delta} (z - h) \partial_x p.$$

437 The solution which satisfies the boundary conditions (5.12g) and (5.12k) is

$$438 \quad (5.16) \quad A_{xz} = \frac{\partial_x p}{1 + \alpha^2/\delta} \left\{ z - h + \alpha \frac{\cosh\left(\frac{\sqrt{1+\alpha^2/\delta}}{\alpha}(z-h)\right) - \cosh\left(\frac{\sqrt{1+\alpha^2/\delta}}{\alpha}z\right)}{\sqrt{1 + \alpha^2/\delta} \sinh\left(\frac{\sqrt{1+\alpha^2/\delta}}{\alpha}h\right)} \right\}.$$

440 Since  $\partial_z p = 0$  in the film, then the normal stress boundary conditions determines that

$$441 \quad (5.17) \quad \partial_x p = -S_p \partial_x^3 h.$$

442 The solution for  $u$  is then

$$443 \quad (5.18) \quad u = \frac{1}{(1 + \alpha^2/\delta)} \frac{S_p}{\text{De}} \partial_x^3 h \left\{ -\left(\frac{z^2}{2} - zh\right) \right. \\ \left. + \frac{\delta}{1 + \alpha^2/\delta} \left[ 1 + \frac{\sinh\left(\frac{\sqrt{1+\alpha^2/\delta}}{\alpha}(z-h)\right) - \sinh\left(\frac{\sqrt{1+\alpha^2/\delta}}{\alpha}z\right)}{\sinh\left(\frac{\sqrt{1+\alpha^2/\delta}}{\alpha}h\right)} \right] \right\}.$$

446 The evolution of the free boundary  $h(x, t)$  is given by

$$447 \quad (5.19) \quad \partial_t h + \partial_x q = 0, \quad q = \int_0^h u \, dz,$$

448 with

$$449 \quad (5.20) \quad q = \frac{1}{1 + \alpha^2/\delta} \frac{S_p}{\text{De}} \left\{ \frac{h^3}{3} + \frac{\delta h}{1 + \alpha^2/\delta} \left[ 1 + \frac{2\alpha \left(1 - \cosh\left(\frac{\sqrt{1+\alpha^2/\delta}}{\alpha}h\right)\right)}{\sqrt{1 + \alpha^2/\delta} h \sinh\left(\frac{\sqrt{1+\alpha^2/\delta}}{\alpha}h\right)} \right] \right\} \partial_x^3 h.$$

450 This complicated equation for the flux is the integral of  $u$  across the film where  $u$  has the potential to develop  
451 boundary layers if  $\alpha$  is small enough. When  $\alpha$  is not vanishingly small, then the flow near the boundaries  
452 still contributes significantly to the flux.

453 If we now take the sharp interface limit  $\alpha \rightarrow 0$  in (5.20), we recover the previously obtained thin film  
454 model (5.10). In this case, the flow away from the boundaries gives the dominant contribution to the flux  $q$   
455 inside the film due to the vanishing width of the boundary layers. Thus, for  $\delta = O(1)$  fixed, the order of the  
456 limits  $\alpha \ll 1$  and  $\epsilon \ll 1$  is immaterial regarding whether slip arises in the resulting thin film equations.

457 **5.2. Large stress diffusion.** For the materials considered in this study, the typical parameter regimes  
458 are covered by the above asymptotic cases, see Table 1. However, further asymptotic regimes that account  
459 for large slip are possible. One of these cases, with large diffusion, is treated now. In this case we see from  
460 (5.12b) that  $u \sim \delta$ . We therefore rescale

$$461 \quad (5.21) \quad (u, w) = \delta(\bar{u}, \bar{w}), \quad t = \frac{\bar{t}}{\delta},$$

462 but keep the same scaling for  $A_{xz}$  and  $A_{zz}$ .

463 For conservation of mass we then have

$$464 \quad (5.22a) \quad \partial_x u + \partial_z w = 0.$$

465 For momentum conservation,

$$466 \quad (5.22b) \quad \epsilon \alpha^2 \delta \text{DeRe} D_t u = -\partial_x p + \alpha^2 \text{De} (\epsilon^2 \partial_x^2 u + \partial_z^2 u) + \epsilon \partial_x A_{xx} + \partial_z A_{xz},$$

$$467 \quad (5.22c) \quad \epsilon^3 \alpha^2 \delta \text{DeRe} D_t w = -\partial_z p + \epsilon^2 \alpha^2 \text{De} (\epsilon^2 \partial_x^2 w + \partial_z^2 w) + \epsilon (\epsilon \partial_x A_{xz} + \partial_z A_{zz}).$$

468 For the polymer part of the deviatoric stress, the equations are as follows.

$$469 \quad (5.22d) \quad \epsilon \delta \text{De} (D_t A_{xx} - 2\epsilon^{-1} A_{xz} \partial_z u - 2\epsilon A_{xx} \partial_x u) + A_{xx} - 1 = \delta (\epsilon^2 \partial_x^2 A_{xx} + \partial_z^2 A_{xx}),$$

$$470 \quad (5.22e) \quad \epsilon \text{De} \delta (D_t A_{xz} - \epsilon^{-1} A_{zz} \partial_z u - \epsilon A_{xx} \partial_x w) + A_{xz} = \delta (\epsilon^2 \partial_x^2 A_{xz} + \partial_z^2 A_{xz}),$$

$$471 \quad (5.22f) \quad \epsilon \text{De} \delta (D_t A_{zz} - 2A_{zz} \partial_z w - 2\epsilon A_{xz} \partial_x w) + A_{zz} - 1 = \delta (\epsilon^2 \partial_x^2 A_{zz} + \partial_z^2 A_{zz}).$$

472 Note that our choice of large pressure i.e. of the scaling  $G_0/\epsilon$  for  $p'$  in (2.2) makes it larger than the leading  
473 order  $A_{zz}$  term.

474 The boundary conditions are, at  $z = 0$ ,

$$475 \quad (5.22g) \quad u = w = 0 \quad \text{and} \quad \partial_z A_{ij} = 0,$$

476 with  $i = x, z$  and  $j = x, z$ .

477 We now turn to the free surface boundary conditions at  $z = h(x, t)$ . We have

$$478 \quad (5.22h) \quad \mathbf{n} = (-\epsilon \partial_x h \mathbf{i} + \mathbf{j}) N^{-1}, \quad \mathbf{t} = (\mathbf{i} + \epsilon \partial_x h \mathbf{j}) N^{-1}, \quad \text{and} \quad N = \sqrt{1 + (\epsilon \partial_x h)^2}.$$

479 On the free surface  $z = h$ ,

$$480 \quad (5.22i) \quad \partial_t h - u \partial_x h = w;$$

481

$$482 \quad -S_p \frac{\partial_x^2 h}{[1 + \epsilon^2 (\partial_x h)^2]^{3/2}} = p + \frac{1}{1 + \epsilon^2 h_x^2} \left\{ -\epsilon [A_{zz} - 1 + \epsilon^2 (\partial_x h)^2 (A_{xx} - 1)] \right. \\ 483 \quad \left. - 2\alpha^2 \text{De} \epsilon^2 \partial_x h (\partial_z u + \epsilon^2 \partial_x w) \right. \\ 484 \quad \left. - 2\epsilon \partial_x h A_{xz} + 2\alpha^2 \text{De} \epsilon^2 [\partial_z w + \epsilon^2 (\partial_x h)^2 \partial_x u] \right\};$$

485

$$486 \quad 0 = \epsilon \partial_x h (A_{zz} - A_{xx}) + A_{xz} [1 - \epsilon^2 (\partial_x h)^2] \\ 487 \quad (5.22k) \quad + \alpha^2 \text{De} (\partial_z u + \epsilon^2 \partial_x w) [1 - \epsilon^2 (\partial_x h)^2] - 2\alpha^2 \text{De} \epsilon \partial_x h (\partial_x u - \partial_z w);$$

488 and

$$489 \quad (5.22l) \quad (\partial_z A_{ij} - \epsilon^2 \partial_x h \partial_x A_{ij}) N^{-1} = 0.$$

490 **5.2.1. Leading order equations.** We consider the  $O(1)$  problem for  $\epsilon \ll 1$  and  $\delta \gg 1$ , keeping  $\alpha$   
491 fixed. For conservation of mass we have

$$492 \quad (5.23) \quad \partial_x u + \partial_z w = 0.$$

493 For momentum conservation,

$$494 \quad (5.24) \quad 0 = -\partial_x p + \alpha^2 \text{De} \partial_z^2 u + \partial_z A_{xz},$$

$$495 \quad (5.25) \quad 0 = \partial_z p,$$

496 where, for the sake of simplicity, we have also assumed that  $\text{DeRe} \ll 1$ . Using the definitions of  $\text{De}$  and  $\text{Re}$ ,  
497 this requires  $U \ll \sqrt{\eta_s/\rho/\lambda} \approx 10^{-3} \text{m/s}$ ; from the values in Table 1 we see that this is readily achieved.

498 For the polymer part of the deviatoric stress, the equations are as follows.

$$499 \quad (5.26) \quad -2\text{De} A_{xz} \partial_z u = \partial_z^2 A_{xx},$$

$$500 \quad (5.27) \quad -\text{De} A_{zz} \partial_z u = \partial_z^2 A_{xz},$$

$$501 \quad (5.28) \quad 0 = \partial_z^2 A_{zz}.$$



502 He we see the consequence of our choice that the pressure is larger than the leading order  $A_{zz}$  term.

503 The boundary conditions are, at  $z = 0$ ,

504 (5.29) 
$$u = w = 0 \text{ and } \partial_z A_{ij} = 0,$$

505 with  $i = x, z$  and  $j = x, z$ .

506 On the free surface  $z = h$ ,

507 (5.30) 
$$\partial_t h - u \partial_x h = w;$$

508

509 (5.31) 
$$-S_p \partial_x^2 h = p$$

510

511 (5.32) 
$$0 = A_{xz} + \alpha^2 \text{De} \partial_z u.$$

512 and

513 (5.33) 
$$\partial_z A_{ij} = 0.$$

514 The solution for  $A_{zz}$  is

515 (5.34) 
$$A_{zz} = A_1(x, t)$$

516 with an unknown (but  $z$ -independent) function  $A_1$ . Furthermore,

517 (5.35) 
$$u = D_1(x, t) \sinh\left(z \frac{\sqrt{A_1(x, t)}}{\alpha}\right) + \frac{\partial_x p}{\text{De} A_1(x, t)} \left[ \cosh\left(z \frac{\sqrt{A_1(x, t)}}{\alpha}\right) - 1 \right],$$

518 
$$A_{xz} = -\alpha \text{De} \sqrt{A_1(x, t)} D_1(x, t) \cosh\left(z \frac{\sqrt{A_1(x, t)}}{\alpha}\right)$$

519 (5.36) 
$$+ \partial_x p \left[ \frac{-\alpha}{\sqrt{A_1(x, t)}} \sinh\left(z \frac{\sqrt{A_1(x, t)}}{\alpha}\right) + z - h \right].$$

520

521  $D_1$  can be eliminated from these solutions by using (5.33), resulting in

522 (5.37) 
$$D_1(x, t) = \frac{\partial_x p}{\text{De} A_1(x, t)} \frac{1 - \cosh\left(h \frac{\sqrt{A_1(x, t)}}{\alpha}\right)}{\sinh\left(h \frac{\sqrt{A_1(x, t)}}{\alpha}\right)}.$$

523 Letting  $\alpha \rightarrow 0$  we find

524 (5.38) 
$$D_1 \rightarrow -\frac{\partial_x p}{\text{De} A_1(x, t)}.$$

525 Using this in (5.35) yields (in the same limit)

526 (5.39) 
$$u(x, t) = -\frac{\partial_x p}{\text{De} A_1(x, t)}.$$

527 **5.2.2. Next order problem: Distinguished limit  $1/\delta = d\epsilon$ .** To determine  $A_1(x, t)$ , we need to  
 528 consider the next order problem. For this purpose we assume the distinguished limit  $1/\delta = d\epsilon$  with

529 
$$d = \frac{1}{\delta\epsilon} = O(1).$$

530 For simplicity let  $\text{Re} \ll 1$  be negligible. In the bulk, we only need to consider (5.22f), which becomes

531 (5.40) 
$$\text{De} (\epsilon D_t A_{zz} - 2\epsilon A_{zz} \partial_z w - 2\epsilon^2 A_{xz} \partial_x w) + d\epsilon (A_{zz} - 1) = \epsilon^2 \partial_x^2 A_{zz} + \partial_z^2 A_{zz}.$$

532 Its boundary conditions are, at  $z = 0$ ,

$$533 \quad (5.41) \quad \partial_z A_{zz} = 0,$$

534 and at  $z = h(x, t)$ ,

$$535 \quad (5.42) \quad (\partial_z A_{ij} - \epsilon^2 \partial_x h \partial_x A_{ij}) N^{-1} = 0.$$

536 Now expand with a regular series in powers of  $\epsilon$ ,

$$537 \quad A_{zz} = A_{zz}^{(0)} + \epsilon A_{zz}^{(1)} + \dots,$$

538 and similarly for the other variables. Leading order is as for the moderate  $\delta$  case (simply insert (0) super-  
539 scripts). To next order we obtain, for the polymer stress equation,

$$540 \quad (5.43) \quad \text{De}(D_t A_{zz}^{(0)} - 2A_{zz}^{(0)} \partial_z w^{(0)}) + d(A_{zz}^{(0)} - 1) = \partial_z^2 A_{zz}^{(1)};$$

542 and for the boundary conditions at  $z = 0$  and  $z = h(x, t)$ ,

$$543 \quad (5.44) \quad \partial_z A_{zz}^{(1)} = 0.$$

544 We then substitute the solution from (5.34) into (5.43) and integrate with respect to  $z$  from 0 to  $h(x, t)$ ;  
545 using the boundary conditions yields the solvability condition

$$546 \quad (5.45) \quad \partial_t A_1 + u \partial_x A_1 + 2A_1 \partial_x u + \frac{d}{\text{De}}(A_1 - 1) = 0,$$

547 where we have omitted the superscripts from  $u$ . Note that  $u$  from (5.39) is independent of  $z$  so that mass  
548 conservation yields

$$549 \quad (5.46) \quad \partial h + \partial_x(uh) = 0.$$

550 Combining equations (5.31), (5.39), (5.45), (5.46) gives the system

$$551 \quad (5.47a) \quad \partial_t A_1 + \frac{S_p}{\text{De}} \left[ 2\partial_x^4 h - \partial_x^3 h \frac{\partial_x A_1}{A_1} \right] + \frac{d}{\text{De}}(A_1 - 1) = 0,$$

$$552 \quad (5.47b) \quad \partial_t h + \frac{S_p}{\text{De}} \partial_x \left( \frac{h \partial_x^3 h}{A_1} \right) = 0.$$

553

We note that in the limit  $d \gg 1$ , we obtain  $A_1 \equiv 1$  and thus get from (5.47b)

$$\partial_t h + \frac{S_p}{\text{De}} \partial_x (h \partial_x^3 h) = 0.$$

554 This is the same evolution equation that results from the  $\delta \rightarrow \infty$  limit of (5.10) after rescaling time according  
555 to (5.21). We now turn to solving a simple example problem from this system.

556 **5.2.3. Linear stability of the uniform solution.** To gain some insight into the large stress diffusion  
557 model, we consider sinusoidal disturbances to the temporally- and spatially-uniform solutions  $h = A_1 = 1$  on  
558 an infinite domain. We find that these uniform states are stable, so this is analogous to the leveling problem  
559 [25]. We may write

$$560 \quad (5.48) \quad h(x, t) = 1 + \tilde{\epsilon} \mathcal{H}(t) e^{ikx} \quad \text{and} \quad A_1(x, t) = 1 + \tilde{\epsilon} \mathcal{A}(t) e^{ikx},$$

561 where  $\tilde{\epsilon} \ll 1$  and the amplitudes  $\mathcal{H}$  and  $\mathcal{A}$  may be complex valued (we omitted the complex conjugate term  
562 for simplicity). The initial values of the amplitudes are  $\mathcal{A}(0) = \mathcal{A}_0$ , and  $\mathcal{H}(0) = \mathcal{H}_0$ . Substitution into  
563 equations (5.47a) and (5.47b), keeping terms of  $O(\tilde{\epsilon})$  only, results in the following linear system of ODEs for  
564 the amplitude:

$$565 \quad (5.49a) \quad \dot{\mathcal{A}} + \frac{2S_p k^4}{\text{De}} \mathcal{H} + \frac{d}{\text{De}} \mathcal{A} = 0,$$

$$566 \quad (5.49b) \quad \dot{\mathcal{H}} + \frac{S_p k^4}{\text{De}} \mathcal{H} = 0.$$

567

568 The dots denote time derivatives. Solving this system gives

$$569 \quad (5.50a) \quad \mathcal{A}(t) = \left( \mathcal{A}_0 - \mathcal{H}_0 \frac{2S_p k^4}{S_p k^4 - d} \right) \exp\left(-\frac{d}{\text{De}} t\right) + \mathcal{H}_0 \frac{2S_p k^4}{S_p k^4 - d} \exp\left(-\frac{S_p k^4}{\text{De}} t\right),$$

$$570 \quad (5.50b) \quad \mathcal{H}(t) = \mathcal{H}_0 \exp\left(-\frac{S_p k^4}{\text{De}} t\right).$$

571  
572 Note that the terms proportional to  $\mathcal{H}_0$  that appear in 5.50a are in phase provided that  $S_p k^4 - d > 0$ , that  
573 is, for sufficiently short waves; otherwise they are out of phase with the wavenumber-independent polymer  
574 stress decay rate.

575 There are two time scales for decay for this linearized problem. One is  $d/\text{De}$  from internal polymer stress  
576 relaxation, and the other is  $S_p k^4/\text{De}$  which is from surface tension. The polymer stress relaxation scale is  
577 faster if  $k < k_c = (d/S_p)^{1/4}$ . Using the values from Table 1, for CTAB 25/25 and for CPyCl/NaSal 50/25,  
578 we have  $k_c \sim 100$ , so that for any long wave situation the polymer stress relaxation will be faster than the  
579 capillarity-driven decay. If we use  $H = 10^{-5}\text{m}$  and  $\ell = 10^{-3}\text{m}$ , then  $k_c \sim 10$ , and a similar conclusion may  
580 be drawn. For  $k = 1$ ,  $d/\text{De} \gg S_p/\text{De}$  and the time scales differ by about seven orders of magnitude for  
581 CPyCl/NaSal 50/25; the scales differ by orders of magnitude for all materials in Table 1.

582 **6. Discussion and Outlook.** In this paper we have considered planar channel flow and thin film free  
583 surface flows governed by a diffusive upper convected Maxwell model of a micelle solution with a Newtonian  
584 solvent. For a pressure driven channel flow the flow structure and dynamics, namely the formation of  
585 boundary layers and the transitions in the flow field, are controlled by two parameters: The ratio of the  
586 solvent viscosity to the zero shear rate polymer viscosity  $\eta_s/\eta_0 = 1/(1 + \eta_0^p/\eta_s)$ , and the non-dimensional  
587 stress diffusion parameter  $\delta$ . Since usually  $\eta_s/\eta_0^p \ll 1$ , this ratio can also be considered instead of the former.  
588 We have shown that this viscosity ratio together with  $\delta$  control the thickness of the boundary layer  $\alpha$ , while  
589 the magnitude of  $\delta$  determines the magnitude of the *apparent slip*.

590 This connection can be rationalized by treating the channel flow (or the thin film flow) as a two-layer  
591 flow, with a bulk flow near the center (or near the free surface, respectively) and thin layer of width  $\alpha$  at the  
592 boundaries (or the substrate).

593 As shown in a study of bi-layer thin film models by Jachalski et al. [14], the flow in a layer of viscosity  
594  $\eta_2$  on top of another layer of height  $h_1$  and much smaller viscosity  $\eta_1$  adjacent to a substrate experiences an  
595 *apparent slip* of  $h_1/(\eta_1/\eta_2)$ .

596 In fact, effective viscosities  $\eta_{\text{eff}}^{\text{center}}$  and  $\eta_{\text{eff}}^{\text{layer}}$  can be obtained for each of these regions from the ratio  
597  $A'_{xz}/\partial_{z'} u'$  as  $z' \rightarrow 0$  and  $z' \rightarrow -H/2$ ,

$$598 \quad \eta_{\text{eff}}^{\text{center}} = \lim_{z' \rightarrow 0} \frac{A'_{xz}}{\partial_{z'} u'} = \eta_p^0, \quad \eta_{\text{eff}}^{\text{layer}} = \lim_{z' \rightarrow -H/2} \frac{A'_{xz}}{\partial_{z'} u'} = \eta_p^0 \frac{\alpha}{2\delta},$$

599 where the limits have been evaluated by using (3.2) and (3.3) together with the scalings and definitions (2.2)  
600 and (2.3), assuming that  $\delta$  is fixed and  $\alpha \ll 1$  (which follows from  $\eta_p^0 \gg \eta_s$  and  $\delta$  fixed). Thus, using  $\eta_{\text{eff}}^{\text{layer}}$   
601 for  $\eta_1$  and  $\eta_{\text{eff}}^{\text{center}}$  for  $\eta_2$ , and  $h_1 = \alpha$ , we obtain the apparent slip-length for the outer channel flow

$$602 \quad \frac{\alpha}{\eta_{\text{eff}}^{\text{layer}}/\eta_{\text{eff}}^{\text{center}}} = 2\delta,$$

603 i.e. the same value we obtained previously from (3.6) and the  $\alpha \rightarrow 0$  limit of (3.3).

604 The limit  $\alpha \rightarrow 0$  was also considered for thin films with a free capillary surface and thin-film models  
605 were derived both for the case of moderate ( $\delta$  fixed) and large ( $\delta = O(\varepsilon^{-1})$ ) stress diffusion. Interestingly,  
606 these models show several parallels with those derived earlier in the context of a liquid layer of polymer melt  
607 dewetting from hydrophobized substrate using a Navier-slip condition for slip-lengths of various orders of  
608 magnitude; see Münch et al. [20, 22] and Fetzer et al. [10].

609 Here, the distinction between the two cases is similar to what was found for thin-film models with weak  
610 and strong slip in [22], confirming the association of slip with the parameter  $\delta$  also in the case of thin film  
611 flows. Due to the choice of the regime for the Deborah number  $\text{De}$ , the models correspond to those expected  
612 for a Newtonian rheology in the bulk. In contrast to [22], however, the models here correspond to slip laws  
613 with a slip length that has a singular dependence on the film profile  $h$ .

614 Our analysis of the sharp-interface limit  $\alpha \rightarrow 0$  and the derivation of several thin-film models for the  
 615 simplest type of model of micelle solutions suggest further investigations into other regimes of Deborah num-  
 616 ber, in particular in the case of large stress diffusion, where corresponding strong-slip type thin film models  
 617 even for full nonlinear viscoelastic rheologies [21] can be expected. Further work will consider extensions of  
 618 our stability analysis for these models together with numerical solutions of the thin-film models.

### 619 **Appendix A. Matching to the inner solution at $z = h$ .**

620 We now determine  $A_{zz}$ , which is in fact the leading order approximation of the outer solution, i.e.  $A_{zz}^{(0)}$ .  
 621 Matching also requires the next order correction to the inner problem near  $z = h$ . In terms of the inner  
 622 variables near  $z = h$ ,

$$623 \quad \zeta = \frac{h(x, t) - z}{\alpha},$$

624 we obtain to next order in  $\alpha$  the problem

$$625 \quad (\text{A.1a}) \quad 0 = \partial_x \tilde{u}^{(0)} + \partial_x h \partial_x \tilde{u}^{(1)} - \partial_\zeta \tilde{w}^{(1)},$$

$$626 \quad 0 = -\partial_x \tilde{p}^{(0)} - \partial_x h \partial_\zeta \tilde{p}^{(1)} + \frac{\text{De}}{\delta} (1 + \varepsilon^2 (\partial_x h)^2) \partial_\zeta^2 \tilde{u}^{(0)} - \partial_\zeta \tilde{A}_{xz}^{(1)} \\ 627 \quad (\text{A.1b}) \quad + \varepsilon \partial_x \tilde{A}_{xx}^{(0)} + \varepsilon \partial_x h \partial_\zeta \tilde{A}_{xx}^{(1)},$$

$$628 \quad 0 = \partial_\zeta \tilde{p}^{(1)} + \frac{\text{De}}{\delta} \varepsilon^2 (1 + \varepsilon^2 (\partial_x h)^2) \partial_\zeta^2 \tilde{w}^{(0)} - \varepsilon \partial_\zeta \tilde{A}_{zz}^{(1)} \\ 629 \quad (\text{A.1c}) \quad + \varepsilon^2 \partial_x \tilde{A}_{xz}^{(0)} + \varepsilon^2 \partial_x h \partial_\zeta \tilde{A}_{xz}^{(1)},$$

$$630 \quad (\text{A.1d}) \quad \partial_\zeta^2 \tilde{A}_{xx}^{(1)} = \frac{\text{De}}{\delta} \frac{2}{1 + \varepsilon^2 (\partial_x h)^2} \left( \tilde{A}_{xz}^{(0)} - \varepsilon \partial_x h \tilde{A}_{xx}^{(0)} \right) \partial_\zeta \tilde{u}^{(0)},$$

$$631 \quad (\text{A.1e}) \quad \partial_\zeta^2 \tilde{A}_{xz}^{(1)} = \frac{\text{De}}{\delta} \frac{1}{1 + \varepsilon^2 (\partial_x h)^2} \left( \tilde{A}_{zz}^{(0)} \partial_\zeta \tilde{u}^{(0)} - \varepsilon^2 \partial_x h \tilde{A}_{xx}^{(0)} \partial_\zeta \tilde{w}^{(0)} \right),$$

$$632 \quad (\text{A.1f}) \quad \partial_\zeta^2 \tilde{A}_{zz}^{(1)} = \frac{\text{De}}{\delta} \frac{2\varepsilon}{1 + \varepsilon^2 (\partial_x h)^2} \left( \tilde{A}_{zz}^{(0)} - \varepsilon \partial_x h \tilde{A}_{xz}^{(0)} \right) \partial_\zeta \tilde{w}^{(0)}.$$

633 At the free surface,  $\zeta = 0$ ,

$$634 \quad (\text{A.1g}) \quad \partial_x h \tilde{u}^{(1)} = \tilde{w}^{(1)},$$

$$635 \quad 0 = \tilde{p}^{(1)} + \frac{\text{De}}{\delta} 2\varepsilon^2 \left( \partial_x h \partial_\zeta \tilde{u}^{(0)} - \partial_\zeta \tilde{w}^{(0)} \right) \\ 636 \quad (\text{A.1h}) \quad + \frac{\varepsilon}{1 + \varepsilon^2 (\partial_x h)^2} \left( \varepsilon (\partial_x h)^2 \tilde{A}_{xx}^{(1)} + 2\varepsilon \partial_x h \tilde{A}_{xz}^{(1)} - \tilde{A}_{zz}^{(1)} \right),$$

$$637 \quad 0 = \varepsilon \partial_x h \left( \tilde{A}_{zz}^{(1)} - \tilde{A}_{xx}^{(1)} \right) \\ 638 \quad + \left[ \tilde{A}_{xz}^{(1)} + \frac{\text{De}}{\delta} \left( -\partial_\zeta \tilde{u}^{(0)} + \varepsilon^2 \partial_x h \partial_\zeta \tilde{w}^{(0)} \right) \right] (1 - \varepsilon^2 (\partial_x h)^2)$$

$$639 \quad (\text{A.1i}) \quad - \frac{\text{De}}{\delta} 2\varepsilon \partial_x h \left( \partial_x h \partial_\zeta \tilde{u}^{(0)} + \partial_\zeta \tilde{w}^{(0)} \right),$$

$$640 \quad (\text{A.1j}) \quad \partial_\zeta \tilde{A}_{ij}^{(1)} = - \frac{\varepsilon^3 \partial_x h}{1 + \varepsilon^2 (\partial_x h)^2} \partial_x \tilde{A}_{ij}^{(0)}.$$

641 This problem can be simplified by introducing the new variables

$$642 \quad (\text{A.2}) \quad \tilde{q}^{(0)} = \partial_x h \tilde{u}^{(0)} - \tilde{w}^{(0)} \quad \text{and} \quad \tilde{r}^{(0)} = \tilde{u}^{(0)} + \varepsilon^2 \partial_x h \tilde{w}^{(0)}.$$

643 instead of  $\tilde{u}^{(0)}$  and  $\tilde{w}^{(0)}$ . Using these variables, we obtain

$$644 \quad (\text{A.3a}) \quad 0 = \partial_\zeta \tilde{q}^{(0)},$$

$$645 \quad 0 = -\partial_x \tilde{p}^{(0)} - \partial_x h \partial_\zeta \tilde{p}^{(1)} + \frac{\text{De}}{\delta} \partial_\zeta^2 \tilde{r}^{(0)} - \partial_\zeta \tilde{A}_{xx}^{(1)}$$

$$646 \quad (\text{A.3b}) \quad + \varepsilon \partial_x \tilde{A}_{xx}^{(0)} + \varepsilon \partial_x h \partial_\zeta \tilde{A}_{xx}^{(1)},$$

$$647 \quad 0 = \partial_\zeta \tilde{p}^{(1)} + \frac{\text{De}}{\delta} \frac{1 + \varepsilon^2 (\partial_x h)^2}{\partial_x h} \partial_\zeta^2 \tilde{r}^{(0)} - \varepsilon \partial_\zeta \tilde{A}_{zz}^{(1)}$$

$$648 \quad (\text{A.3c}) \quad + \varepsilon^2 \partial_x \tilde{A}_{xz}^{(0)} + \varepsilon^2 \partial_x h \partial_\zeta \tilde{A}_{xz}^{(1)},$$

$$649 \quad (\text{A.3d}) \quad \partial_\zeta^2 \tilde{A}_{xx}^{(1)} = \frac{\text{De}}{\delta} \frac{2}{(1 + \varepsilon^2 (\partial_x h)^2)^2} \left( \tilde{A}_{xz}^{(0)} - \varepsilon \partial_x h \tilde{A}_{xx}^{(0)} \right) \partial_\zeta \tilde{r}^{(0)},$$

$$650 \quad (\text{A.3e}) \quad \partial_\zeta^2 \tilde{A}_{xz}^{(1)} = \frac{\text{De}}{\delta} \frac{1}{(1 + \varepsilon^2 (\partial_x h)^2)^2} \left( \tilde{A}_{zz}^{(0)} - \varepsilon^2 (\partial_x h)^2 \tilde{A}_{xx}^{(0)} \right) \partial_\zeta \tilde{r}^{(0)},$$

$$651 \quad (\text{A.3f}) \quad \partial_\zeta^2 \tilde{A}_{zz}^{(1)} = \frac{\text{De}}{\delta} \frac{2 \varepsilon \partial_x h}{(1 + \varepsilon^2 (\partial_x h)^2)^2} \left( \tilde{A}_{zz}^{(0)} - \varepsilon \partial_x h \tilde{A}_{xz}^{(0)} \right) \partial_\zeta \tilde{r}^{(0)}.$$

652 The boundary conditions at  $\zeta = 0$  become:

$$653 \quad (\text{A.3g}) \quad \partial_x h \tilde{u}^{(1)} = \tilde{w}^{(1)},$$

$$654 \quad (\text{A.3h}) \quad 0 = \tilde{p}^{(1)} + \frac{\varepsilon}{1 + \varepsilon^2 (\partial_x h)^2} \left( \varepsilon (\partial_x h)^2 \tilde{A}_{xx}^{(1)} + 2 \varepsilon \partial_x h \tilde{A}_{xz}^{(1)} - \tilde{A}_{zz}^{(1)} \right),$$

$$655 \quad 0 = \varepsilon \partial_x h \left( \tilde{A}_{zz}^{(1)} - \tilde{A}_{xx}^{(1)} \right) + \tilde{A}_{xz}^{(1)} (1 - \varepsilon^2 (\partial_x h)^2)$$

$$656 \quad (\text{A.3i}) \quad - \frac{\text{De}}{\delta} \frac{[1 - \varepsilon^2 (\partial_x h)^2]^2 + 4 \varepsilon (\partial_x h)^2}{1 + \varepsilon^2 (\partial_x h)^2} \partial_\zeta \tilde{r}^{(0)},$$

$$657 \quad (\text{A.3j}) \quad \partial_\zeta \tilde{A}_{ij}^{(1)} = - \frac{\varepsilon^3 \partial_x h}{1 + \varepsilon^2 (\partial_x h)^2} \partial_x \tilde{A}_{ij}^{(0)}.$$

658 Adding (A.3b) to (A.3c) multiplied by  $\partial_x h$ , we obtain

$$659 \quad \frac{\text{De}}{\delta} [2 + \varepsilon^2 (\partial_x h)^2] \partial_\zeta^2 \tilde{r}^{(0)} = \varepsilon \partial_x h \left( \partial_\zeta \tilde{A}_{zz}^{(1)} - \partial_\zeta \tilde{A}_{xx}^{(1)} \right) + [1 - \varepsilon^2 (\partial_x h)^2] \partial_\zeta \tilde{A}_{xz}^{(1)}$$

$$660 \quad (\text{A.4}) \quad + \partial_x \tilde{p}^{(0)} - \varepsilon \partial_x \tilde{A}_{xx}^{(0)} - \varepsilon^2 \partial_x h \partial_x \tilde{A}_{xz}^{(0)}$$

661 We note that from (A.3d)-(A.3f)

$$662 \quad (\text{A.5}) \quad \varepsilon \partial_x h \left( \partial_\zeta^2 \tilde{A}_{zz}^{(1)} - \partial_\zeta^2 \tilde{A}_{xx}^{(1)} \right) + (1 - \varepsilon^2 (\partial_x h)^2) \partial_\zeta^2 \tilde{A}_{xz}^{(1)}$$

$$663 \quad = \frac{\text{De}}{\delta} \frac{1}{1 + \varepsilon^2 (\partial_x h)^2} \left[ \tilde{A}_{zz}^{(0)} - 2 \varepsilon \partial_x h \tilde{A}_{xz}^{(0)} + \varepsilon^2 (\partial_x h)^2 \tilde{A}_{xx}^{(0)} \right] \partial_\zeta \tilde{r}^{(0)}$$

664 Integration with respect to  $\zeta$  and using (A.3j) and (A.4) we obtain the following ordinary differential  
665 equation for  $\tilde{r}^{(0)}$ :

$$666 \quad (\text{A.6}) \quad (1 + \varepsilon^2 (\partial_x h)^2) (2 + \varepsilon^2 (\partial_x h)^2) \partial_\zeta^2 \tilde{r}^{(0)} = \left( \tilde{A}_{zz}^{(0)} - 2 \varepsilon \partial_x h \tilde{A}_{xz}^{(0)} + \varepsilon^2 (\partial_x h)^2 \tilde{A}_{xx}^{(0)} \right) \tilde{r}^{(0)} + f(x, t),$$

667 where

$$668 \quad (\text{A.7}) \quad f(x, t) = \frac{\delta}{\text{De}} (1 + \varepsilon^2 (\partial_x h)^2) \left( \partial_x \tilde{p}^{(0)} - \varepsilon \partial_x \tilde{A}_{xx}^{(0)} - \varepsilon^2 \partial_x h \partial_x \tilde{A}_{xz}^{(0)} \right)$$

$$669 \quad - \left[ \tilde{A}_{zz}^{(0)} - 2 \varepsilon \partial_x h \tilde{A}_{xz}^{(0)} + \varepsilon^2 (\partial_x h)^2 \tilde{A}_{xx}^{(0)} \right] \tilde{r}^{(0)} \Big|_{\zeta=0}$$

$$670 \quad - \frac{\delta}{\text{De}} \left\{ \varepsilon^4 (\partial_x h)^2 \left( \partial_x \tilde{A}_{zz}^{(0)} - \partial_x \tilde{A}_{xx}^{(0)} \right) + \varepsilon^3 \partial_x h [1 - \varepsilon^2 (\partial_x h)^2] \partial_x \tilde{A}_{xz}^{(0)} \right\}.$$

671 The general solution to the second order linear differential equation (A.6) is composed of a particular  
672 solution,

$$673 \quad \tilde{r}_p^{(0)} = - \frac{f(x, t)}{\tilde{A}_{zz}^{(0)} - 2 \varepsilon \partial_x h \tilde{A}_{xz}^{(0)} + \varepsilon^2 (\partial_x h)^2 \tilde{A}_{xx}^{(0)}}$$

674 and an exponentially growing and an exponentially decaying complementary solution, provided that

$$675 \quad (\text{A.8}) \quad \tilde{A}_{zz}^{(0)} - 2\varepsilon \partial_x h \tilde{A}_{xz}^{(0)} + \varepsilon^2 (\partial_x h)^2 \tilde{A}_{xx}^{(0)} > 0.$$

676 (This is satisfied if we restrict our attention to flows that do not deviate much from channel flow, so that  
677  $\tilde{A}_{zz}^{(0)} \sim 1$  and  $\varepsilon$  is small.) The exponentially growing solution is not matchable, and hence that contribution  
678 has been eliminated. Then, for  $\zeta \rightarrow \infty$ ,  $\tilde{r}^0$  tends to  $r_p^{(0)}$ , so we match this to the combination  $u^{(0)} + \varepsilon^2 \partial_x h w^{(0)}$   
679 of the leading order outer solutions. The matching condition can then be solved for  $f(x, t)$  and from this  
680 and (A.7) we obtain  $\tilde{r}^{(0)}|_{\zeta=0}$  in terms of the outer solutions. Now we can integrate (A.1f) once with respect  
681 to  $\zeta$  and then use (A.1j) as well as the information about  $\tilde{r}^{(0)}|_{\zeta=0}$  we just obtained to fix the integration  
682 constants. The resulting expression

$$683 \quad \partial_\zeta \tilde{A}_{zz}^{(1)} = \varepsilon^2 \times O(1) \text{ terms}$$

684 can be matched to the outer solution, which gives a Neumann condition for the outer  $A_{zz}$ ,

$$685 \quad (\text{A.9}) \quad \partial_z A_{zz}^{(0)} \Big|_{z=h} = \varepsilon^2 \times O(1) \text{ terms,}$$

686 with a right hand side that (after matching) only depends on leading order variables of the outer solution.  
687 Here, we do not need the precise form of the right hand side as our goal is to justify (5.11). Indeed, (A.9)  
688 reduces to (5.11) in the limit  $\varepsilon \rightarrow 0$ .

## 689 References.

- 690 [1] N. P. ADHIKARI AND J. L. GOVEAS, *Effects of slip on the viscosity of polymer melts*, J. Polymer Sci.:  
691 Part B: Polymer Physics, 42 (2004), pp. 1888–1904.
- 692 [2] A. AJDARI, *Slippage at a polymer/polymer interface: Entanglements and associated friction*, C.R. Acad.  
693 Sci., Ser. II, 317 (1993), pp. 1159–1163.
- 694 [3] A. AJDARI, F. B. WYART, P. G. DE GENNES, L. LEIBLER, J. VIOVY, AND M. RUBINSTEIN, *Slippage*  
695 *of an entangled polymer melt on a grafted surface*, Physica A, 204 (1994), pp. 17–39.
- 696 [4] P. BALLESTA, G. PETEKIDIS, L. ISA, W. C. K. POON, AND R. BESSEING, *Wall slip and flow of*  
697 *concentrated hard-sphere colloidal suspensions*, J. Rheol., 56 (2012), p. 1005.
- 698 [5] A. BHARDWAJ, E. MILLER, AND J. ROTHSTEIN, *Filament stretching and capillary breakup extensional*  
699 *rheometry measurements of viscoelastic wormlike micelle solutions*, J. Rheol., 51 (2007), pp. 693–719.
- 700 [6] F. BROCHARD-WYART AND P. DE GENNES, *Shear-dependent slippage at a polymer/solid interface*,  
701 Langmuir, 8 (1992), pp. 3033–3037.
- 702 [7] F. BROCHARD-WYART AND P. DE GENNES, *Sliding molecules at a polymer/polymer interface*, C. R.  
703 Acad. Sci. Ser. II, 327 (1993), pp. 13–17.
- 704 [8] M. CROMER, L. P. COOK, AND F. MCKINLEY, *Pressure-driven flow of wormlike micellar solutions in*  
705 *rectilinear microchannels*, J. of Non-Newtonian Fluid Mech., 166 (2011), pp. 180–193.
- 706 [9] A. EL-KAREH AND G. LEAL, *The existence of solutions for all Deborah numbers for non-Newtonian*  
707 *fluids*, J. Non-Newtonian Fluid Mech., 33 (1989), pp. 257–287.
- 708 [10] R. FETZER, K. JACOBS, A. MÜNCH, B. WAGNER, AND T. P. WITELSKI., *New slip regimes and the*  
709 *shape of dewetting thin liquid films.*, Phys. Rev. Lett., 95 (2005), p. 127801.
- 710 [11] S. FIELDING, *Complex dynamics of shear banded flows*, Soft Matter, 2 (2007), pp. 1262–1279.
- 711 [12] H. P. GREENSPAN, *On the motion of a small viscous droplet that wets a surface*, Journal of Fluid  
712 Mechanics, 84 (1978), pp. 125–143.
- 713 [13] C. HUH AND L. SCRIVEN, *Hydrodynamic model of steady movement of a solid/liquid/fluid contact line*,  
714 Journal of Colloid and Interface Science, 35 (1971), pp. 85–101.
- 715 [14] S. JACHALSKI, A. MÜNCH, AND B. WAGNER, *Thin-film models for viscoelastic liquid bi-layers*. WIAS  
716 Preprint 2187, 2015.
- 717 [15] S. M. L. BÉCU AND A. COLIN, *Spatiotemporal dynamics of wormlike micelles under shear*, Phys. Rev.  
718 Lett., 93 (2004), p. 018301.
- 719 [16] E. LAUGA, M.P.BRENNER, AND H. STONE, *Microfluidics: The no-slip boundary condition*, in Hand-  
720 book of Experimental Fluid Dynamics, Springer, New York, 2007, pp. 1219–1240.
- 721 [17] L. LÉGER, *Friction mechanisms and interfacial slip at fluid-solid interfaces*, J. Phys.: Condensed Matter,  
722 15 (2003), pp. S19–S29.

- 723 [18] M. P. LETTINGA AND S. MANNEVILLE, *Competition between shear banding and wall slip in wormlike*  
724 *micelles*, Phys. Rev. Lett., 103 (2009), p. 248302.
- 725 [19] C. MASSELON, A. COLIN, AND P. D. OLMSTED, *Influence of boundary conditions and confinement on*  
726 *nonlocal effects in flows of wormlike micellar systems*, Physical Review E, 81 (2010), p. 021502.
- 727 [20] A. MÜNCH AND B. WAGNER, *Contact-line instability of dewetting thin films*, Physica D, 209 (2005),  
728 pp. 178–190.
- 729 [21] A. MÜNCH, B. WAGNER, M. RAUSCHER, AND R. BLOSSEY, *A thin-film model for corotational Jeffreys*  
730 *fluids under strong slip*, The European Physical Journal E, 20 (2006), pp. 365–368.
- 731 [22] A. MÜNCH, B. WAGNER, AND T. P. WITELSKI, *Lubrication models with small to large slip lengths*, J.  
732 Engr. Math., 53 (2006), pp. 359–383.
- 733 [23] P. NEOGI AND C. A. MILLER, *Spreading kinetics of a drop on a rough solid surface*, Journal of Colloid  
734 and Interface Science, 92 (1983), pp. 338–349.
- 735 [24] P. OLMSTED, *Perspectives on shear banding in complex fluids*, Rheol. Acta, 47 (2008), pp. 283–300.
- 736 [25] S. E. ORCHARD, *On surface leveling in viscous liquids and gels*, Appl. Sci. Res. A, 11 (1962), pp. 451–464.
- 737 [26] C. L. P. OLMSTED, O. RADULESCU, *Johnson-segalman model with a diffusion term in cylindrical*  
738 *couette flow*, J. Rheol., 44 (2000), pp. 257–275.
- 739 [27] P. A. VASQUEZ, G. H. MCKINLEY, AND P. L. COOK, *A network scission model for wormlike micellar*  
740 *solutions*, Journal of Non-Newtonian Fluid Mechanics, 144 (2007), pp. 122–139.
- 741 [28] L. ZHOU, P. VASQUEZ, L. COOK, AND G. H. MCKINLEY, *Modeling the inhomogeneous response and*  
742 *formation of shear bands in steady and transient flows of entangled fluids*, J. Rheol., 32 (2008), pp. 591–  
743 623.